

SUPPLEMENT TO “MITIGATING DISASTER RISKS IN THE AGE OF CLIMATE CHANGE”

(*Econometrica*, Vol. 91, No. 5, September 2023, 1763–1802)

HARRISON HONG

Department of Economics, Columbia University and NBER

NENG WANG

Columbia Business School, Cheung Kong Graduate School of Business, ABFER, and NBER

JINQIANG YANG

School of Finance, Shanghai University of Finance and Economics and Shanghai Institute of International Finance and Economics

APPENDIX OA: MODEL WITH STOCHASTIC DISASTER ARRIVAL RATES

THE DISASTER ARRIVAL RATE in our baseline model of Section 2, while unobservable, is constant. In this section, we generalize the baseline model to allow for the unobservable disaster arrival rate to be stochastic.¹ We assume that the disaster arrival rate follows a two-state continuous-time Markov chain taking two possible values, λ_G in state G and $\lambda_B > \lambda_G$ in state B . Let φ_G denote the transition rate from state G to state B and φ_B denote the transition rate from state B to state G . That is, over a small time period Δt , the transition probability from the G state to the B state is $\varphi_G \Delta t$ and similarly the transition probability from the B state to the G state is $\varphi_B \Delta t$. Our baseline unobservable constant λ model of Section 2 is a special case of this model with $\varphi_G = \varphi_B = 0$.

OA.1. *Model*

As in our baseline model, let π_t denote the conditional probability that the economy is in state B . The belief process $\{\pi_t\}$ evolves as

$$d\pi_t = \mathbb{E}_{t-}[d\pi_t] + \sigma_\pi(\pi_{t-})(d\mathcal{J}_t - \lambda_{t-} dt), \quad (\text{OA.1})$$

where $\sigma_\pi(\pi)$ is given by (8) and $\lambda_{t-} = \lambda_B \pi_{t-} + \lambda_G (1 - \pi_{t-})$ is the expected disaster arrival rate at $t-$ given in (6). Note that the second term is a martingale by construction. Since the economy follows a two-state Markov chain, the expected change of belief is given by

$$\mathbb{E}_{t-}[d\pi_t] = (\varphi_G - (\varphi_B + \varphi_G)\pi_{t-}) dt.$$

We can thus rewrite (OA.1) as follows:

$$d\pi_t = (\varphi_G - (\varphi_B + \varphi_G)\pi_{t-}) dt + \sigma_\pi(\pi_{t-})(d\mathcal{J}_t - \lambda_{t-} dt). \quad (\text{OA.2})$$

Harrison Hong: hh2679@columbia.edu

Neng Wang: neng.wang@columbia.edu

Jinqiang Yang: yang.jinqiang@mail.sufe.edu.cn

¹See also Bayesian learning models of Ghaderi, Kilic, and Seo (2022) and Wachter and Zhu (2021).

Equation (OA.2) implies that π_t in our generalized model is no longer a martingale. This is in sharp contrast with our baseline model (with constant arrival rate), where belief π_t given in (7) is a martingale. Rewriting the drift term in (OA.2), we see that the expected change of belief π_t in our generalized learning model is given by the difference between $\varphi_G(1 - \pi_{t-})$, which is the transition rate out of state G , φ_G , multiplied by $1 - \pi_{t-}$, the conditional probability in state G , and $\varphi_B\pi_t$, which is the transition rate out of state B , φ_B , multiplied by π_{t-} , the conditional probability in state B .²

We note that the jump martingale term (the second term in (OA.2)) in our generalized model is the same as in the belief updating process (7) for our baseline model. As a result, when a disaster strikes at t , the belief immediately increases from the pre-jump level π_{t-} to $\pi_t = \pi^\mathcal{J}$ by $\sigma_\pi(\pi_{t-})$, where $\pi^\mathcal{J}$ is given by (9), the same as in our baseline model with unobservable constant arrival rate λ .

Taking these results together, absent jump arrivals (i.e., $d\mathcal{J}_t = 0$), we obtain the following expression for the rate at which belief changes, $\widehat{\mu}_\pi(\pi_{t-}) = d\pi_t/dt$:

$$\widehat{\mu}_\pi(\pi) = (\varphi_G - (\varphi_B + \varphi_G)\pi) - \pi(1 - \pi)(\lambda_B - \lambda_G). \quad (\text{OA.3})$$

Generalizing the unobservable λ from a constant to a stochastic process (two-state Markov chain) does not change the belief updating upon the immediate arrival of a jump. However, belief updating conditional on no-jump arrival is different from the baseline case with unobservable constant arrival rate λ .

Next, we calculate the posterior belief π_t at t conditional on no-jump arrival over the time interval (s, t) , that is, $dJ_v = 0$ for $s < v \leq t$. Using (OA.2) and integrating $\{\pi_v; v \in (s, t)\}$ from s to t conditional on no jump over the interval (s, t) , we obtain the following function:

$$\pi_t = \pi_s - \frac{2(\delta_0\pi_s^2 + \delta_1\pi_s + \delta_2)(e^{-\sqrt{\delta_1^2 - 4\delta_0\delta_2}(t-s)} - 1)}{(\sqrt{\delta_1^2 - 4\delta_0\delta_2} + \delta_1 + 2\delta_0\pi_s)(e^{-\sqrt{\delta_1^2 - 4\delta_0\delta_2}(t-s)} - 1) + 2\sqrt{\delta_1^2 - 4\delta_0\delta_2}}, \quad (\text{OA.4})$$

where $\delta_0 = -(\lambda_G - \lambda_B)$, $\delta_1 = \lambda_G - \lambda_B - (\varphi_G + \varphi_B)$, and $\delta_2 = \varphi_G$. For our baseline model ($\varphi_G = \varphi_B = 0$), π_t in (OA.4) can be simplified to (11).

In Figure O-1, we plot the belief process $\{\pi_t : t \in (0, 20)\}$ conditional on no-jump arrival, which means $d\mathcal{J}_v = 0$ where $v \in (0, t) = (0, 20)$, for three cases: (1) the stationary case with $\varphi_G = \varphi_B = 2\%$ (the solid line); (2) the case with $\varphi_G = 2\%$ and $\varphi_B = 0$, where the economy is eventually absorbed at the B state, (the dotted line); and (3) the baseline constant λ case as $\varphi_G = \varphi_B = 0$ (the dashed line). The prior for the low value of λ is set at $\pi_0 = 0.08$ for all three cases.

First, for the two cases with stochastic λ , π_t decreases with t even absent jump arrivals. For example, the solid line (for the $\varphi_G = \varphi_B = 2\%$ case) shows that π_t slowly decreases to 0.0277 in 20 years absent jump arrivals. For the other case where the B state is absorbing ($\varphi_B = 0$), π_t decreases to 0.0285 at $t = 20$ absent jumps (the dotted line.) The belief dynamics for these two cases with stochastic λ are similar to the dynamic for our constant unobservable λ model (the dashed line), which shows that π_t decreases over time to zero and the agent becomes more optimistic (the no news is good news result), and the only difference is the long-run mean absent jump arrivals. So long as the transition rates φ_G and φ_B are small (which is the practically relevant case), our baseline model (with constant

²As a result, when $\pi_t = 0$ (in the G state for sure), the drift of belief π_t is exactly φ_G , the arrival rate from the G to the B state. Similarly, by symmetry, when $\pi_t = 1$ (in the B state for sure), the drift is exactly $-\varphi_B$.

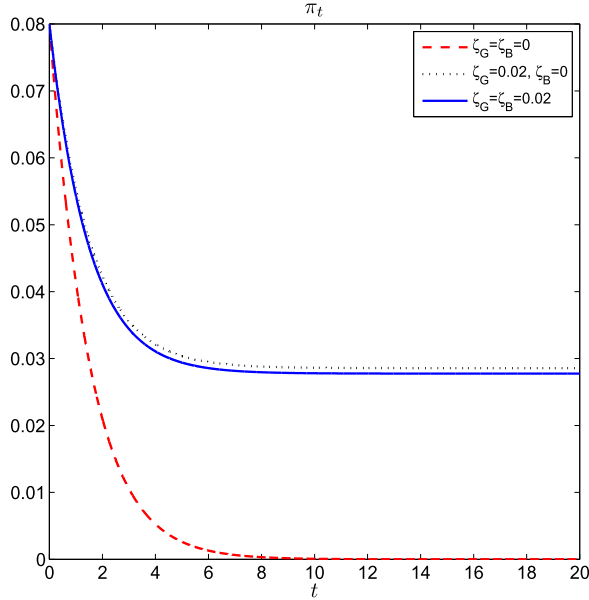


FIGURE O-1.—This figure plots the time series of π_t absent jumps in our generalized model, where the jump arrival rate, λ , is unobservable and follows a two-state Markov chain taking on two possible values ($\lambda_G = 0.1$ and $\lambda_B = 0.8$) with a prior of $\pi_0 = 0.08$ that the current value of λ is λ_B . Our baseline model with constant unobservable λ corresponds to $\varphi_G = \varphi_B = 0$ (the dashed line).

unobservable λ) and the stochastic unobservable λ model generate similar quantitative predictions. For parsimony, we use the constant λ model for our quantitative analysis in the paper.

OA.2. Solution

Using the belief process $\{\pi_{tj}\}$ given in (OA.2), we obtain the following HJB equation for the planner's allocation problem:

$$0 = \max_{\mathbf{C}, \mathbf{I}, \mathbf{x}^e, \mathbf{x}^d} f(\mathbf{C}, V) + (\mathbf{I} - \delta_K \mathbf{K}) V_{\mathbf{K}}(\mathbf{K}, \pi) + \widehat{\mu}_{\pi}(\pi) V_{\pi}(\mathbf{K}, \pi) + \frac{1}{2} \sigma_K^2 \mathbf{K}^2 V_{\mathbf{K}\mathbf{K}}(\mathbf{K}, \pi) + \lambda(\pi) \mathbb{E}^{\mathbf{x}^d} [V((1 - N(\mathbf{x}^e)(1 - Z))\mathbf{K}, \pi^J) - V(\mathbf{K}, \pi)], \quad (\text{OA.5})$$

where $\widehat{\mu}_{\pi}(\pi)$ is given in (OA.3). The FOCs for aggregate investment \mathbf{I} , (scaled) aggregate disaster distribution mitigation spending \mathbf{x}^d , and (scaled) aggregate disaster exposure mitigation spending \mathbf{x}^e are the same as those for our baseline model (with constant unobservable λ), which are given in (14), (15), and (16), respectively.

Substituting the value function $V(\mathbf{K}, \pi)$ given in (17) and its derivatives into the HJB equation (OA.5), using the three FOCs ((14), (15), and (16)), and simplifying these equations, we obtain the four-equation ODE system for $b(\pi)$, $\mathbf{i}(\pi)$, $\mathbf{x}^d(\pi)$, and $\mathbf{x}^e(\pi)$, given

in

$$0 = \frac{\rho}{1 - \psi^{-1}} \left[\left[\frac{b(\pi)}{\rho(1 + \phi'(\mathbf{i}(\pi)))} \right]^{1-\psi} - 1 \right] + \mathbf{i}(\pi) - \delta_K - \frac{\gamma \sigma_K^2}{2} + \widehat{\mu}_\pi(\pi) \frac{b'(\pi)}{b(\pi)} \\ + \frac{\lambda(\pi)}{1 - \gamma} \left[\left(\frac{b(\pi^\mathcal{J})}{b(\pi)} \right)^{1-\gamma} \mathbb{E}^{\mathbf{x}^d(\pi)} \left((1 - N(\mathbf{x}^e(\pi))(1 - Z))^{1-\gamma} \right) - 1 \right] \quad (\text{OA.6})$$

and (19)–(21) for $\pi \in (0, 1)$. The key difference between (OA.6) and the ODE (18) for $b(\pi)$ in our baseline model (with constant but unobservable λ) is that the drift of π absent jumps, $\widehat{\mu}_\pi(\pi)$ given in (OA.3), appears in (OA.6) while $\mu_\pi(\pi)$ given in (10) appears in the ODE (18).³ The other three equations for $\mathbf{i}(\pi)$, $\mathbf{x}^d(\pi)$ and $\mathbf{x}^e(\pi)$ for our stochastic λ model are (19), (20), and (21), the same as those for our baseline model of Section 3. The boundary conditions at the $\pi = 0$ and $\pi = 1$ states are implied by the preceding equations.

Next, we summarize the solution for our generalized learning model.

PROPOSITION O-1: *The first-best solution for our generalized learning model is given by the value function (17) and the quartet policy rules, $b(\pi)$, $\mathbf{i}(\pi)$, $\mathbf{x}^d(\pi)$, and $\mathbf{x}^e(\pi)$, where $0 \leq \pi \leq 1$, via the four-equation ODE system ((OA.6), (19), (20), and (21)).*

OA.3. Quantitative Analysis

Next, we analyze the solutions for our generalized model with stochastic unobservable λ . For the stochastic λ model, we set both the transition rate from state G to B (φ_G) and that from state B to G (φ_B) to 2%, that is, $\varphi_G = \varphi_B = 1/50 = 2\%$, which imply an average duration of 50 years for both G and B states. In the long run, the economy is in either state G or B with equal (50%) probability. To ease exposition and facilitate comparison with our baseline (constant unobservable λ) model, we keep all other parameter values unchanged.

In Figure O-2, we plot (scaled) public mitigation $\mathbf{x}^d(\pi)$ (panel A), (scaled) private mitigation $\mathbf{x}^e(\pi)$ (panel B), investment-capital ratio $\mathbf{i}(\pi)$ (panel C), and consumption-capital $\mathbf{c}(\pi)$ (panel D) as functions of belief π for the planner's first-best solutions: the solid lines are for the baseline constant λ model and the dashed lines are for the stochastic λ model.

Panels A and B show that for both public mitigation $\mathbf{x}^d(\pi)$ and private exposure mitigation $\mathbf{x}^e(\pi)$ are significantly lower for the stochastic λ model, and this is intuitive because the agent is exposure to less uncertainty about the belief due the mean reversion of π in the stochastic λ model, which induces less mitigation motivation. Quantitatively, the differences for investment and consumption are of very small (second- and third-order effects, as we can see from the scale for the vertical axes in panels C and D.) This is because the transition of λ occurs once every 50 years on average.

Note that investment and consumption are even flatter (less responsive to changes of belief) in the stochastic λ model than in the constant λ model. Figure O-3 corroborates the belief mean reversion effect on welfare, growth, and valuation by showing that the welfare measure, the WTP $\zeta_p(\pi)$ (panel A), the expected growth rate $\mathbf{g}(\pi)$ (panel C), Tobin's average q , and the risk-free rate $r(\pi)$ are all smoother (flatter) as functions of π in the stochastic λ model than in the constant λ model.

³The wedge $\widehat{\mu}_\pi(\pi) - \mu_\pi(\pi) = (\varphi_G - (\varphi_B + \varphi_G)\pi)$ precisely captures the effect of stochastic transition between the G and B states.

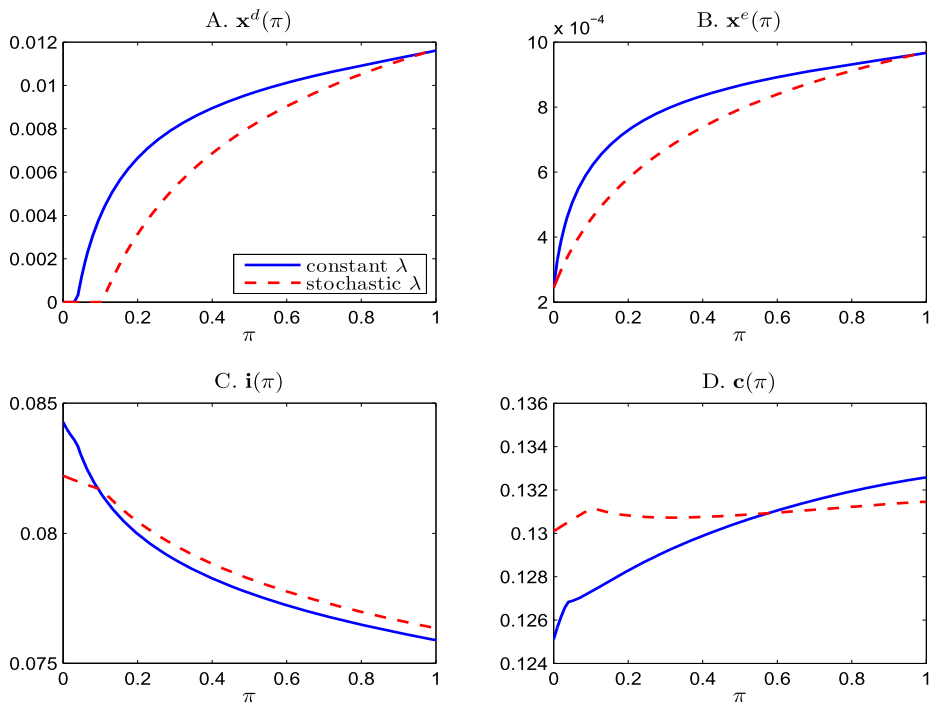


FIGURE O-2.—This figure compares two learning models: the constant λ and the stochastic λ models. The transition rates are $\varphi_G = \varphi_B = 0.02$ for the stochastic λ model (solid lines). The transition rates are $\varphi_G = \varphi_B = 0$ for our baseline (constant λ) model (dashed lines).

The intuition is as follows. As belief mean reversion in the stochastic λ model, the agent is less optimistic in the low- π state but also less pessimistic in the high- π state, in the stochastic λ model, that is, compared with the constant λ model. As a result, the planner reduces both consumption and investment in response to changes of belief (so that the planner better smoothes investment/consumption across states and over time.)

In sum, our analysis shows that for plausible values of slow belief mean reversion, the quantitative results of our learning model (with stochastic λ) are similar to those of our learning model (with constant λ). And we confirm the intuition that belief mean reversion reduces the impact of learning on welfare, valuation, and policy rules.

APPENDIX OB: EXTERNAL HABIT MODEL

In this [Appendix](#), we solve the model with external habit (Campbell–Cochrane) preferences (Section 7.7) and provide a quantitative analysis.⁴

⁴An alternative to the external habit model analyzed in this section is to specify an internal habit formation model as in [Jermann \(1998\)](#). Due to space constraints, we leave the internal habit formation model out.

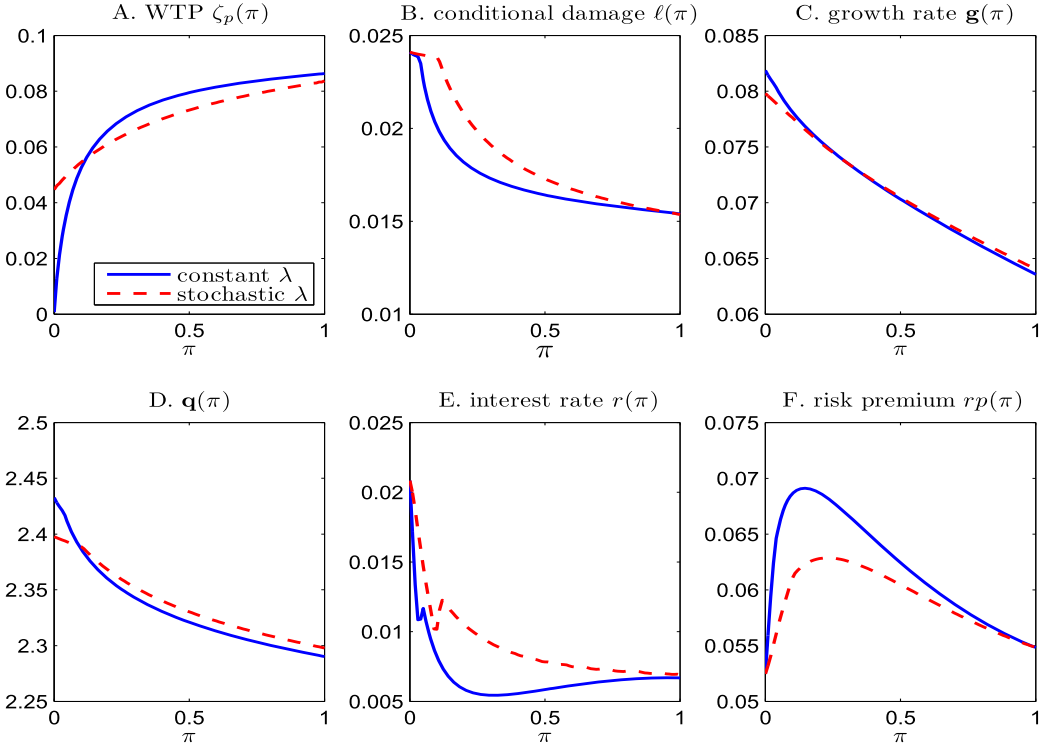


FIGURE O-3.—This figure compares two learning models: the constant λ and the stochastic λ models. The transition rates are $\varphi_G = \varphi_B = 0.02$ for the stochastic λ model (solid lines). The transition rates are $\varphi_G = \varphi_B = 0$ for our baseline (constant λ) model (dashed lines).

OB.1. Model

The representative agent has a nonexpected utility over consumption $\{C_t; t \geq 0\}$ relative to a stochastic habit process $\{\mathcal{H}_t; t \geq 0\}$ (Campbell and Cochrane (1999)) given by

$$\mathbb{E} \left(\int_0^\infty \rho e^{-\rho t} U(C_t, \mathcal{H}_t) dt \right),$$

where $\rho > 0$ is the time rate of preference, $U(C, \mathcal{H}) = \frac{(C - \mathcal{H})^{1-\gamma}}{1-\gamma}$, and $\gamma > 0$ is a curvature parameter. It is convenient to work with S_t , the surplus consumption ratio at t defined as

$$S_t = \frac{C_t - \mathcal{H}_t}{C_t}.$$

Let s_t be its natural logarithm: $s_t = \ln(S_t)$. As in Campbell and Cochrane (1999) and this literature, we assume that s_t follows a mean-reverting process with stochastic volatility:

$$ds_t = (1 - \kappa_s)(\bar{s} - s_t) dt + \delta(s_t) \sigma_K d\mathcal{W}_t^K, \quad (\text{OB.7})$$

where $\bar{s} > 0$ is the steady-state value of s_t and κ_s measures the degree of persistence.⁵ The function $\delta(s_t)$ in (OB.7) is the same sensitivity function as the one in Campbell and Cochrane (1999). The production side of the economy and the learning model are the same as in our baseline model of Section 2.

Planner's Solution. The (log) surplus consumption ratio $\{s_t; t \geq 0\}$ acting as the exogenous preferences shock is the new state variable. Let $V(\mathbf{K}, \pi, s)$ denote the household's value function. The following HJB equation characterizes the planner's optimal resource allocation:

$$\begin{aligned} \rho V = & \max_{c, \mathbf{I}, \mathbf{x}^e, \mathbf{x}^d} \rho \frac{(\mathbf{C}e^s)^{1-\gamma}}{1-\gamma} + (\mathbf{I} - \delta_K \mathbf{K})V_{\mathbf{K}} + \mu_{\pi}(\pi)V_{\pi} + (1 - \kappa_s)(\bar{s} - s)V_s \\ & + \frac{\sigma_K^2 \mathbf{K}^2 V_{\mathbf{K}\mathbf{K}}}{2} + \frac{1}{2} \sigma_K^2 \delta(s)^2 V_{ss} + \sigma_K^2 \delta(s) \mathbf{K} V_{\mathbf{K}s} \\ & + \lambda(\pi) \mathbb{E}^{\mathbf{x}^d} [V((1 - N(\mathbf{x}^e)(1 - Z))\mathbf{K}, \pi^{\mathcal{J}}, s) - V(\mathbf{K}, \pi, s)]. \end{aligned} \quad (\text{OB.8})$$

Unlike in our baseline model with the Epstein–Zin utility, the agent now not only takes into account the evolution of s (via the drift term involving V_s and the quadratic-variation term involving V_{ss}), but also has incentives to hedge against shocks to the surplus consumption ratio (via the quadratic-covariation term involving $V_{\mathbf{K}s}$).

We show that the value function $V(\mathbf{K}, \pi, s)$ is homogeneous with degree $(1 - \gamma)$ in \mathbf{K} :

$$V(\mathbf{K}, \pi, s) = \frac{1}{1 - \gamma} (b(\pi, s)\mathbf{K})^{1-\gamma}, \quad (\text{OB.9})$$

where $b(\pi, s)$ is a measure of welfare proportional to the certainty equivalent wealth under optimality. (To ease comparison, we still use b as the function for the welfare measure here but with the understanding that the b function for the external habit model depends on both π and s and differs from the b function for our baseline Epstein–Zin model.)

Importantly, unlike the welfare measure $(b(\pi))$ in our baseline model (Section 3), $b(\pi, s)$ in our external habit model depends on not only belief π but also the (log) surplus consumption ratio s . Our external habit model is technically more challenging than our baseline model with Epstein–Zin utility, as the external habit becomes an additional state variable in addition to capital stock and belief.⁶

In (OB.7), $\delta(s_t)$ is the sensitivity function proportional to the conditional volatility of ds_t in response to $d\mathcal{W}_t^K$, which we assume is given by the following square-root function:

$$\delta(s) = \frac{1}{\bar{S}} \sqrt{1 - 2(s - \bar{s})} - 1, \quad s \leq s_{\max}$$

and $\delta(s) = 0$ for $s > s_{\max}$, where $s_{\max} = \bar{s} + \frac{1-\bar{S}^2}{2}$ and $\bar{S} = e^{\bar{s}}$.⁷

⁵We write $1 - \kappa_s$ as the rate of mean reversion as in Campbell and Cochrane (2015). The higher the value of κ_s , the more persistent the s_t process. The $\kappa_s = 1$ special case corresponds to a unit-root process.

⁶Because of the homogeneity property of the Epstein–Zin utility, only capital stock and belief are state variables after simplifying the model solution.

⁷Additionally, we set $\bar{S} = \sigma_K \sqrt{\frac{\gamma}{1-\kappa_s}}$ as in Campbell and Cochrane (1999).

OB.2. *Solution*

Substituting the value function given in (OB.9) into the HJB equation (OB.8), we obtain

$$\begin{aligned}
0 = & \max_{c, i, \mathbf{x}^e, \mathbf{x}^d} \frac{\rho}{1-\gamma} \left[\left(\frac{\mathbf{c}(\pi, s) e^s}{b(\pi, s)} \right)^{1-\gamma} - 1 \right] + (\mathbf{i}(\pi, s) - \delta_K) + \mu_\pi(\pi) \frac{b_\pi(\pi, s)}{b(\pi, s)} \\
& + (1 - \kappa_s)(\bar{s} - s) \frac{b_s(\pi, s)}{b(\pi, s)} - \frac{\gamma \sigma_K^2}{2} + \frac{\sigma_K^2 \delta(s)^2}{2} \left(\frac{b_{ss}(\pi, s)}{b(\pi, s)} - \gamma \frac{(b_s(\pi, s))^2}{b(\pi, s)^2} \right) \\
& + (1 - \gamma) \sigma_K^2 \delta(s) \frac{b_s(\pi, s)}{b(\pi, s)} \\
& + \frac{\lambda(\pi)}{1-\gamma} \left[\left(\frac{b(\pi^\mathcal{J}, s)}{b(\pi, s)} \right)^{1-\gamma} \mathbb{E}^{\mathbf{x}^d} \left((1 - N(\mathbf{x}^e(\pi, s))(1 - Z))^{1-\gamma} \right) - 1 \right].
\end{aligned}$$

Using the resource constraint $\mathbf{c} = A - \mathbf{i} - \phi(\mathbf{i}) - \mathbf{x}^d - \mathbf{x}^e$ to simplify the FOC for investment \mathbf{i} , we obtain the ODE system in the region where $\pi \in [0, 1]$ and $s \in (-\infty, s_{\max})$:

$$\begin{aligned}
0 = & \frac{\rho}{1-\gamma} \left[\left(\frac{b(\pi, s) e^{-s}}{\rho(1 + \phi'(\mathbf{i}(\pi, s)))} \right)^{1-\gamma} - 1 \right] + (\mathbf{i}(\pi, s) - \delta_K) + (1 - \kappa_s)(\bar{s} - s) \frac{b_s(\pi, s)}{b(\pi, s)} \\
& + \mu_\pi(\pi) \frac{b_\pi(\pi, s)}{b(\pi, s)} - \frac{\gamma \sigma_K^2}{2} + \frac{\sigma_K^2 \delta(s)^2}{2} \left(\frac{b_{ss}(\pi, s)}{b(\pi, s)} - \gamma \frac{(b_s(\pi, s))^2}{b(\pi, s)^2} \right) \\
& + (1 - \gamma) \sigma_K^2 \delta(s) \frac{b_s(\pi, s)}{b(\pi, s)} \\
& + \frac{\lambda(\pi)}{1-\gamma} \left[\left(\frac{b(\pi^\mathcal{J}, s)}{b(\pi, s)} \right)^{1-\gamma} \mathbb{E}^{\mathbf{x}^d(\pi, s)} \left((1 - N(\mathbf{x}^e(\pi, s))(1 - Z))^{1-\gamma} \right) - 1 \right], \quad (\text{OB.10})
\end{aligned}$$

and

$$\begin{aligned}
b(\pi, s) = & [A - \mathbf{i}(\pi, s) - \phi(\mathbf{i}(\pi, s)) - \mathbf{x}^d(\pi, s) - \mathbf{x}^e(\pi, s)]^{\gamma/(\gamma-1)} \\
& \times [\rho \mathbf{q}(\pi, s)]^{1/(1-\gamma)} e^s, \quad (\text{OB.11})
\end{aligned}$$

$$\begin{aligned}
\frac{1}{\mathbf{q}(\pi, s)} = & \lambda(\pi) \left[\frac{b(\pi^\mathcal{J}, s)}{b(\pi, s)} \right]^{1-\gamma} N'(\mathbf{x}^e(\pi, s)) \mathbb{E}^{\mathbf{x}^d(\pi, s)} \\
& \times [(Z - 1)(1 - N(\mathbf{x}^e(\pi, s))(1 - Z))^{-\gamma}], \quad (\text{OB.12})
\end{aligned}$$

$$\begin{aligned}
\frac{1}{\mathbf{q}(\pi, s)} = & \frac{\lambda(\pi)}{1-\gamma} \left[\frac{b(\pi^\mathcal{J}, s)}{b(\pi, s)} \right]^{1-\gamma} \\
& \times \int_0^1 \left[\frac{\partial \xi(Z; \mathbf{x}^d(\pi, s))}{\partial \mathbf{x}^d} (1 - N(\mathbf{x}^e(\pi, s))(1 - Z))^{1-\gamma} \right] dZ, \quad (\text{OB.13})
\end{aligned}$$

where Tobin's q is given by the standard q -theoretic formula: $\mathbf{q}(\pi, s) = 1 + \phi'(\mathbf{i}(\pi, s))$.

Using the resource constraint $\mathbf{c} = A - \mathbf{i} - \phi(\mathbf{i}) - \mathbf{x}^d - \mathbf{x}^e$ to simplify the FOCs for mitigation spendings, \mathbf{x}^e and \mathbf{x}^d , we obtain the optimal exposure mitigation and distribution

mitigation spending rules, (OB.12) and (OB.13) for \mathbf{x}^e and \mathbf{x}^d , respectively. The boundary conditions at the absorbing states ($\pi = 0$ and $\pi = 1$) are implied by the preceding equations.

At $s = s_{\max}$, we have the following boundary condition:

$$\begin{aligned}
0 = & \frac{\rho}{1-\gamma} \left[\left(\frac{b(\pi, s_{\max}) e^{-s_{\max}}}{\rho(1+\phi'(\mathbf{i}(\pi, s_{\max})))} \right)^{1-\gamma^{-1}} - 1 \right] + (\mathbf{i}(\pi, s_{\max}) - \delta_K) \\
& + (1-\kappa_s)(\bar{s} - s_{\max}) \frac{b_s(\pi, s_{\max})}{b(\pi, s_{\max})} - \frac{\gamma\sigma_K^2}{2} + \mu_\pi(\pi) \frac{b_\pi(\pi, s_{\max})}{b(\pi, s_{\max})} \\
& + \frac{\lambda(\pi)}{1-\gamma} \left[\left(\frac{b(\pi^J, s_{\max})}{b(\pi, s_{\max})} \right)^{1-\gamma} \right. \\
& \left. \times \mathbb{E}^{\mathbf{x}^d(\pi, s_{\max})} \left((1 - N(\mathbf{x}^e(\pi, s_{\max}))(1 - Z))^{1-\gamma} - 1 \right) \right]. \tag{OB.14}
\end{aligned}$$

Additionally, $\mathbf{i}(\pi, s_{\max})$, $\mathbf{x}^e(\pi, s_{\max})$ and $\mathbf{x}^d(\pi, s_{\max})$, satisfy (OB.11)–(OB.13) at $s = s_{\max}$.⁸

We summarize our model's solution in the following proposition.

PROPOSITION O-2: *The first-best solution for our external habit model is given by the value function (OB.9) and the quartet policy rules, $b(\pi, s)$, $\mathbf{i}(\pi, s)$, $\mathbf{x}^d(\pi, s)$, and $\mathbf{x}^e(\pi, s)$, where $0 \leq \pi \leq 1$ and $-\infty < s \leq s_{\max}$, via the four-equation ODE system (OB.10), (OB.11), (OB.12), and (OB.13), together with (OB.14) and (OB.11)–(OB.13) for $s = s_{\max}$.*

Next, we use the planner's solution to derive our model's asset pricing implications.

OB.3. Asset Pricing Implications

Using the planner's solution, we infer the SDF \mathbb{M}_t process by applying Itô's lemma to

$$\mathbb{M}_t = e^{-\rho t} \frac{U_C(C_t, \mathcal{H}_t)}{U_C(C_0, \mathcal{H}_0)} = e^{-\rho t} \left(\frac{C_t S_t}{C_0 S_0} \right)^{-\gamma}.$$

We then use the no-arbitrage restriction for the SDF to obtain the equilibrium risk-free rate, the market price of risk, and the stock market risk premium.

Then using Itô's lemma, we obtain

$$\begin{aligned}
\frac{d\mathbb{M}_t}{\mathbb{M}_t} = & -\rho dt - \gamma \left(\mathbf{i}(\pi, s) - \delta_K - \frac{\sigma_K^2}{2} \right) dt \\
& + (1-\kappa_s)(\bar{s} - s_t) \left((1-\gamma) \frac{b_s(\pi, s)}{b(\pi, s)} - \frac{\mathbf{q}_s(\pi, s)}{\mathbf{q}(\pi, s)} - 1 \right) dt \\
& + \mu_\pi(\pi) \left((1-\gamma) \frac{b_\pi(\pi, s)}{b(\pi, s)} - \frac{\mathbf{q}_\pi(\pi, s)}{\mathbf{q}(\pi, s)} \right) dt
\end{aligned}$$

⁸Note that as $s \rightarrow -\infty$ is not reachable in equilibrium, we can ignore the corresponding boundary conditions for our numerical analysis.

$$\begin{aligned}
& - \left[(1 - \gamma) \frac{b_s(\pi, s)^2}{b(\pi, s)^2} - \frac{\mathbf{q}_s(\pi, s)^2}{\mathbf{q}(\pi, s)^2} \right] \frac{(\sigma_K \delta(s))^2}{2} dt + \frac{\sigma_{\mathbb{M}}(\pi, s)^2}{2} dt \\
& + \left[(1 - \gamma) \frac{b_{ss}(\pi, s)}{b(\pi, s)} - \frac{\mathbf{q}_{ss}(\pi, s)}{\mathbf{q}(\pi, s)} \right] \frac{(\sigma_K \delta(s))^2}{2} dt - \sigma_{\mathbb{M}}(\pi, s) d\mathcal{W}_t^K \\
& + [\eta(\pi, s; Z, \mathbf{x}^e) - 1] d\mathcal{J}_t, \tag{OB.15}
\end{aligned}$$

where $\eta(\pi, s; Z, \mathbf{x}^e) = \frac{\mathbf{q}(\pi, s)}{\mathbf{q}(\pi^{\mathcal{J}}, s)} \left(\frac{b(\pi^{\mathcal{J}}, s)}{b(\pi, s)} \right)^{1-\gamma} (1 - N(\mathbf{x}^e(\pi, s))(1 - Z))^{-\gamma}$ and

$$\sigma_{\mathbb{M}}(\pi, s) = \left[\left(1 + \frac{\mathbf{q}_s(\pi, s)}{\mathbf{q}(\pi, s)} - (1 - \gamma) \frac{b_s(\pi, s)}{b(\pi, s)} \right) \delta(s) + \gamma \right] \sigma_K.$$

Using the equilibrium restriction that the drift of $\frac{dM_t}{M_t}$ equals $-r_{t-} dt$, we obtain

$$\begin{aligned}
r(\pi, s) &= \rho + \gamma \left(\mathbf{i}(\pi, s) - \delta_K - \frac{\sigma_K^2}{2} \right) - (1 - \kappa_s)(\bar{s} - s_t) \left((1 - \gamma) \frac{b_s(\pi, s)}{b(\pi, s)} - \frac{\mathbf{q}_s(\pi, s)}{\mathbf{q}(\pi, s)} - 1 \right) \\
& - \mu_{\pi}(\pi) \left((1 - \gamma) \frac{b_{\pi}(\pi, s)}{b(\pi, s)} - \frac{\mathbf{q}_{\pi}(\pi, s)}{\mathbf{q}(\pi, s)} \right) \\
& + \left[(1 - \gamma) \frac{b_s(\pi, s)^2}{b(\pi, s)^2} - \frac{\mathbf{q}_s(\pi, s)^2}{\mathbf{q}(\pi, s)^2} \right] \frac{(\sigma_K \delta(s))^2}{2} \\
& - \left[(1 - \gamma) \frac{b_{ss}(\pi, s)}{b(\pi, s)} - \frac{\mathbf{q}_{ss}(\pi, s)}{\mathbf{q}(\pi, s)} \right] \frac{(\sigma_K \delta(s))^2}{2} - \frac{\sigma_{\mathbb{M}}(\pi, s)^2}{2} \\
& - \lambda(\pi) [\mathbb{E}^{x^d}(\eta(\pi, s; Z, \mathbf{x}^e)) - 1].
\end{aligned}$$

Applying Itô's lemma to firm value $Q(K, \pi, s) = q(\pi, s)K$ and using (OB.15), we obtain

$$\begin{aligned}
r(\pi, s)q(\pi, s) &= \max_{i, x^e} A - i - \phi(i) - x^e + (i - \sigma_{\mathbb{M}}(\pi, s)\sigma_K)q(\pi, s) + \mu_{\pi}(\pi)q_{\pi}(\pi, s) \\
& + [(1 - \kappa_s)(\bar{s} - s) + \delta(s)\sigma_K^2 - \sigma_{\mathbb{M}}(\pi, s)\delta(s)\sigma_K]q_s(\pi, s) \\
& + \frac{\sigma_K^2 \delta(s)^2}{2} q_{ss}(\pi, s) \\
& + \lambda(\pi) \mathbb{E}^{x^d} [\eta(\pi, s; Z, \mathbf{x}^e) (q(\pi^{\mathcal{J}}, s)(1 - N(x^e)(1 - Z)) - q(\pi, s))].
\end{aligned}$$

Finally, using the equilibrium conditions $q(\pi, s) = \mathbf{q}(\pi, s)$ and $x^e(\pi, s) = \mathbf{x}^e(\pi, s)$, we write

$$\begin{aligned}
\frac{d\mathbf{Q}_t + \mathbf{D}_{t-} dt}{\mathbf{Q}_{t-}} &= \left[\mu_{\mathbf{Q}}(\pi_{t-}, s_{t-}) + \lambda(\pi_{t-}) \left(\frac{\mathbf{Q}_t^{\mathcal{J}}}{\mathbf{Q}_{t-}} - 1 \right) \right] dt \\
& + \left[\frac{\mathbf{q}_s(\pi_{t-}, s_{t-}) \delta(s_{t-})}{\mathbf{q}(\pi_{t-}, s_{t-})} + 1 \right] \sigma_K d\mathcal{W}_t^K \\
& + \left(\frac{\mathbf{Q}_t^{\mathcal{J}}}{\mathbf{Q}_{t-}} - 1 \right) (d\mathcal{J}_t - \lambda(\pi_{t-}) dt),
\end{aligned}$$

where $\frac{\mathbf{Q}_t^{\mathcal{J}}}{\mathbf{Q}_{t-}} = \frac{(1-N(\mathbf{x}_{t-}^e)(1-Z))\mathbf{q}(\pi_t^{\mathcal{J}}, s_{t-})}{\mathbf{q}(\pi_{t-}, s_{t-})}$, and

$$\begin{aligned} \mu_{\mathbf{Q}}(\pi_{t-}, s_{t-}) &= r(\pi_{t-}, s_{t-}) + \sigma_{\mathbb{M}}(\pi_{t-}, s_{t-}) \left(1 + \delta(s_{t-}) \frac{\mathbf{q}_s(\pi_{t-}, s_{t-})}{\mathbf{q}(\pi_{t-}, s_{t-})} \right) \sigma_K \\ &\quad + \lambda(\pi_{t-}) \mathbb{E}^{\mathbf{N}_{t-}^d} \left[\eta(\pi_{t-}, s_{t-}; Z, \mathbf{x}_{t-}^e) \left(1 - \frac{\mathbf{Q}_t^{\mathcal{J}}}{\mathbf{Q}_{t-}} \right) \right]. \end{aligned}$$

The market risk premium is

$$\begin{aligned} \text{rp}(\pi_{t-}, s_{t-}) &= \sigma_{\mathbb{M}}(\pi_{t-}, s_{t-}) \left(1 + \delta(s_{t-}) \frac{\mathbf{q}_s(\pi_{t-}, s_{t-})}{\mathbf{q}(\pi_{t-}, s_{t-})} \right) \sigma_K \\ &\quad - \lambda(\pi_{t-}) \mathbb{E}^{\mathbf{N}_{t-}^d} \left[(\eta(\pi_{t-}, s_{t-}; Z, \mathbf{x}_{t-}^e) - 1) \left(\frac{\mathbf{Q}_t^{\mathcal{J}}}{\mathbf{Q}_{t-}} - 1 \right) \right]. \end{aligned}$$

Next, we calibrate the model and provide a quantitative analysis.

OB.4. Quantitative Analysis

The key new parameter for the external habit model is the (log) surplus consumption parameter κ_s . We set the persistence parameter for external habit at $\kappa_s = 0.87$ per annum as in [Campbell and Cochrane \(1999\)](#). For other parameter values, we borrow from the baseline model to ease exposition.

OB.5. Quantitative Results

In [Figures O-4 and O-5](#), we compare the external habit model at the steady state where $S = \bar{S} = 0.63$ with the Epstein–Zin recursive utility model. Panel A of [Figure O-4](#) shows that the distribution mitigation $\mathbf{x}^d(\pi)$ policies for the two utility models are close to each other. However, panel B of [Figure O-4](#) shows that the exposure mitigation $\mathbf{x}^e(\pi)$ policies for the two models can differ somewhat for intermediate values of π . Nonetheless, our findings based on these two utility models suggest that our main results on how changes of belief impact disaster distribution and exposure adaptation spendings are reasonably robust.

Panel C of [Figure O-4](#) shows that the investment-capital ratio is lower in our Epstein–Zin model than in the external habit model at the steady state where $S = \bar{S} = 0.63$. Panel D of [Figure O-4](#) shows that the consumption-capital ratio is higher in our Epstein–Zin model than in the external habit model, which is expected as the sum of adaptation spending, investment, and consumption is the same and equals the productivity A in these two models.

It is interesting to note that while $\mathbf{i}(\pi)$ decreases with π for the Epstein–Zin utility model, $\mathbf{i}(\pi)$ increases with π in the external habit model. This difference is caused by the long-run risk force in the Epstein–Zin utility specification, where the EIS $\psi > 1$. To generate the prediction that worsening belief (increasing π) lowers Tobin's q and equivalently investment (as investment increases with Tobin's q), we require $\psi > 1$.

The external habit model differs from the baseline Epstein–Zin utility model in two ways. First, risk aversion is significantly enhanced by and also varies with external habit. Second, the EIS implied by our external habit model also generates a time-varying elasticity of intertemporal substitution (EIS). As risk aversion increases with habit stock, the

EIS decreases. This is why our model predicts investment (and hence Tobin's q) increases with belief. Figure O-5 reports the WTP, conditional damage $\ell(\pi)$, the expected growth rate $\mathbf{g}(\pi)$, Tobin's average $q(\pi)$, the risk-free rate $r(\pi)$, and the market risk premium $\text{rp}(\pi)$. While there are some differences, we see that these two models generate similar results when it comes to the importance of adaptations in reducing conditional damage and ensuring growth.

In Figure O-6, we focus on the external habit utility model by comparing two formulations: the planner's first-best economy (solid lines) with the market economy solution (dashed lines). We plot the two mitigation spending, investment, and consumption policies for varying levels of S , for a given belief $\pi_0 = 0.08$.

Panel A of Figure O-6 shows that there is no public mitigation in a competitive market economy for the same externality argument as in our baseline model with Epstein–Zin utility. This panel also shows that \mathbf{x}^d increases as the surplus consumption ratio increases. Similarly, both the exposure mitigation spending and investment increase with S (panels B and C). The intuition for these results is as follows. As we increase S , the marginal utility of consumption (and SDF \mathbb{M}_t) decrease, which causes \mathbf{c} to decrease with S (see panel D). Additionally, the marginal value of investment and that of mitigation (for both types) increase, which causes \mathbf{x}^d , \mathbf{x}^e , and \mathbf{i} to increase with S as shown in panels A, B, and C.

Finally, we note that the private mitigation spending \mathbf{x}^e is larger for the market economy than for the planner's economy. This is because the marginal benefit of private mitigation is higher in the market economy as there is no public mitigation. In contrast, as the public

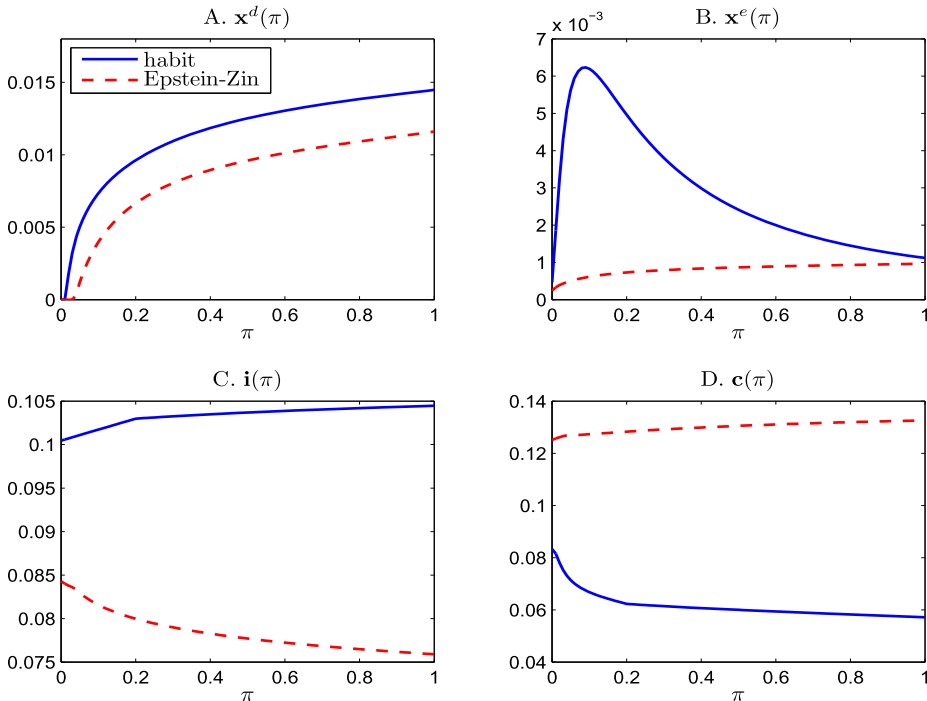


FIGURE O-4.—This figure compares the first-best solutions for the external habit model (solid lines) and the baseline model with Epstein–Zin recursive utility (dashed lines). The parameter values for our baseline (Epstein–Zin) model are summarized in Table 4.

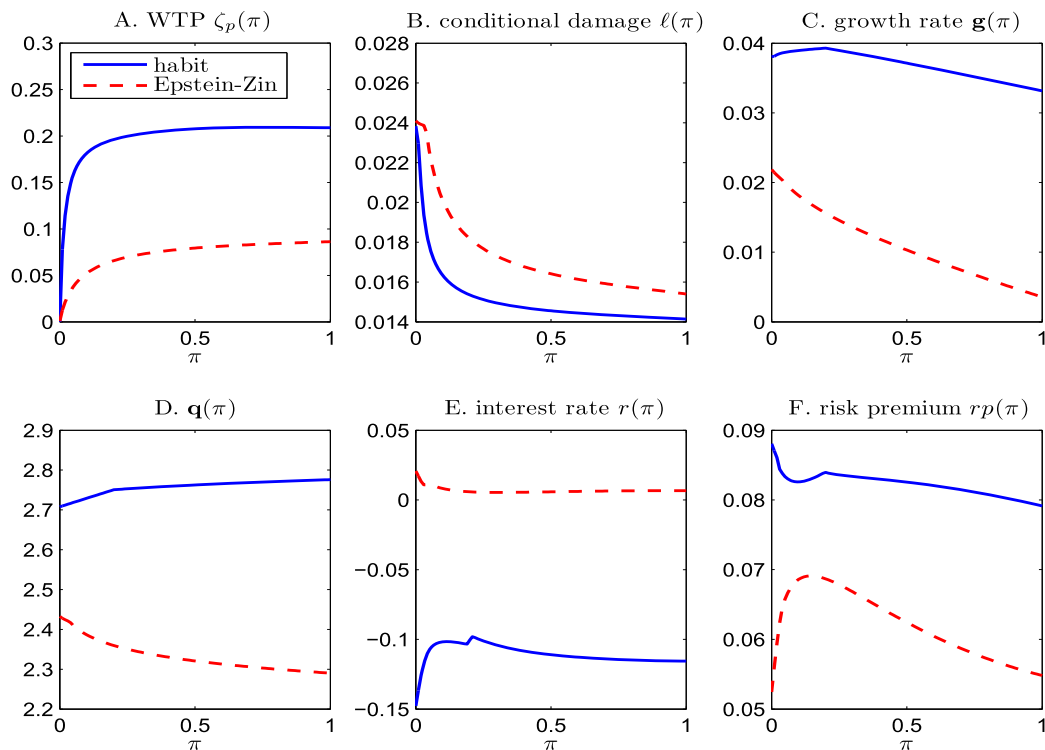


FIGURE O-5.—This figure compares the first-best solutions for the external habit model (solid lines) and the baseline model with Epstein–Zin recursive utility (dashed lines). The parameter values for our baseline (Epstein–Zin) model are summarized in Table 4.

mitigation spending \mathbf{x}^d is positive and significant under the planner’s economy, the additional value of private mitigation spending in the planner’s economy is smaller, and hence \mathbf{x}^e is smaller under the planner’s economy than under the market economy (a substitution effect).

In sum, we show that time-varying risk aversion induced by external habit influences optimal mitigation policies, but the general results that we obtain from our baseline model with Epstein–Zin utility remains valid in our external habit model.

APPENDIX OC: COMPARATIVE STATICS

OC.1. Elasticity of Intertemporal Substitution ψ

In Figure O-7, we plot the first-best solutions for three levels of the EIS ψ : $\gamma = 0.125, 1, 1.5$. Panels A and B show that the lower the EIS ψ , the higher both public mitigation \mathbf{x}^d and private mitigation \mathbf{x}^e spendings. Quantitatively, these differences are not very large. Panel C shows that the lower the EIS ψ , the higher the investment-capital ratio $\mathbf{i}(\pi)$. Panel D shows that the lower the EIS ψ , the lower the consumption-capital ratio $\mathbf{c}(\pi)$, as $\mathbf{c} = A - (\mathbf{i} + \mathbf{x}^d + \mathbf{x}^e)$. Panel E shows that the lower the EIS ψ , the higher Tobin’s average $\mathbf{q}(\pi)$. This follows directly from the comparative static result of changing ψ on \mathbf{i} (panel C), as Tobin’s q is increasing with \mathbf{i} : $\mathbf{q}(\pi) = 1 + \phi'(\mathbf{i}(\pi))$. Panel F shows that the lower the EIS ψ the higher the price-dividend ratio $\mathbf{q}(\pi)/\mathbf{c}(\pi)$, which follows from the comparative effects shown in panels D and E.

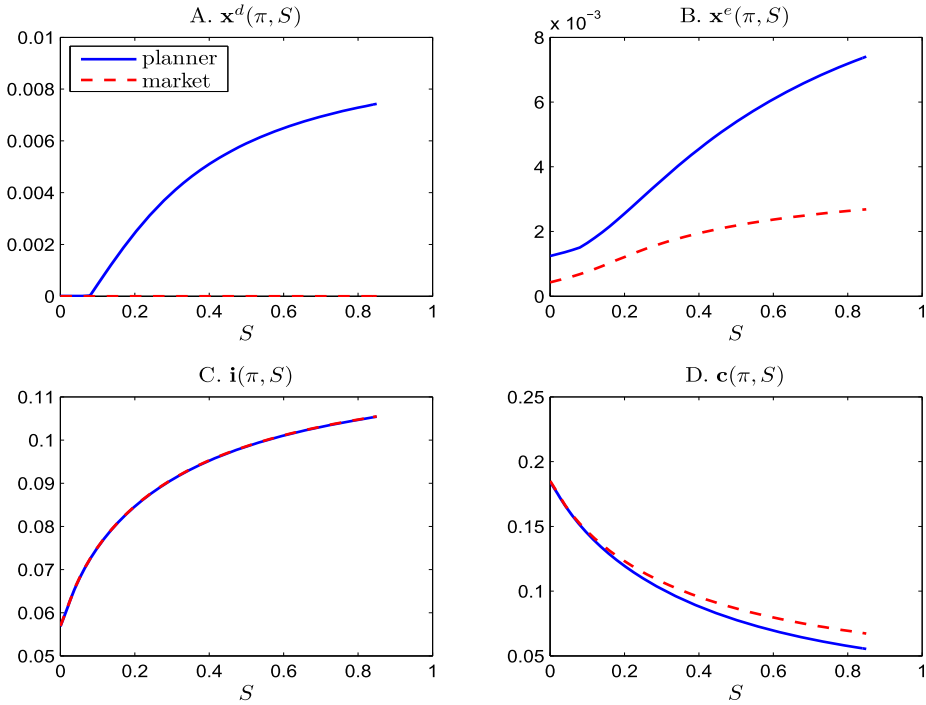


FIGURE O-6.—This figure plots the optimal policies for the first-best economy (solid lines) and the market economy (dashed lines) as functions of surplus consumption ratio S , for the external habit (Campbell—Cochrane) model, where $\pi_0 = 0.08$.

The intuition is as follows. The higher the EIS ψ , the less marginal propensity to consume as in partial equilibrium model consistent with Ramsey/Friedman consumption rule. As a result, the agent spends more on mitigation and also invests more for the future.

Additionally, we show that whether the price-dividend ratio $\mathbf{q}(\pi)/\mathbf{c}(\pi)$ increases or decreases when disaster arrives (which increases (worsens) belief π) crucially depends on whether the EIS ψ is larger or smaller than one. In our baseline case where $\psi = 1.5 > 1$, the equilibrium price-dividend ratio $\mathbf{q}(\pi)/\mathbf{c}(\pi)$ decreases when a disaster arrives (i.e., when π increases). This result is consistent with [Bansal and Yaron \(2004\)](#) and the subsequent long-run risk literature, who show that the price-dividend ratio decreases in response to a negative growth shock when the EIS parameter ψ is set to be larger than one. Unlike Bansal and Yaron's pure exchange economy, our model features production, and hence we need to compute the endogenous dividend \mathbf{c} together with value of capital, Tobin's \mathbf{q} , in order to obtain the price-dividend ratio. However, we obtain the same results for the effect of EIS on the price-dividend ratio.

For the unity EIS ($\psi = 1$) Epstein—Zin utility case, which is a generalized version of expected logarithmic utility (with a flexible choice of risk aversion parameter γ), the wealth and the substitution effects exactly offset each other. As a result, the equilibrium price-dividend ratio remains constant, that is, $\mathbf{q}(\pi)/\mathbf{c}(\pi) = 1/\rho = 20$ at all levels of π (see the dotted line in panel F). Finally, with $\psi = 1/\gamma = 0.125 < 1$, the wealth effect is stronger than the substitution effect. For this case, as belief worsens (increases), the price-dividend ratio $\mathbf{q}(\pi)/\mathbf{c}(\pi)$ increases, which is empirically counterfactual. This is one reason (among

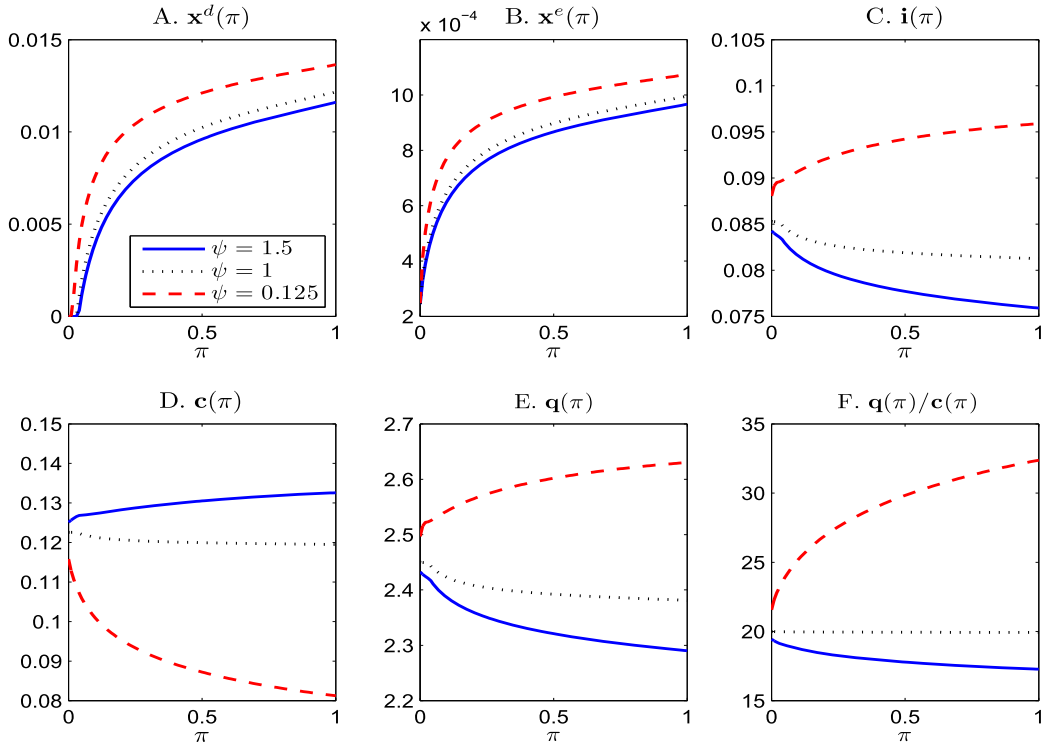


FIGURE O-7.—This figure plots the first-best solution for three values of the EIS ψ : $1/\gamma = 0.125, 1, 1.5$ for our baseline learning model (with Epstein–Zin utility). The other parameter values are given in Table 4.

others) why Epstein–Zin utility with an EIS larger than one ($\psi > 1$) is a more appealing utility specification than commonly used expected utility for asset pricing.

In Figure O-8, we show that the quantitative effects of EIS ψ on the WTP is large (panel A). In panel B, the lower the EIS ψ , the lower the conditional damages $\ell(\pi)$. This is because the agent with a lower EIS mitigates less as we show in panels A and B of Figure O-8. As a result, the lower EIS the lower the conditional damages $\ell(\pi)$. Figure O-9 of panel A shows that the lower the EIS ψ , the higher the expected growth rate $g(\pi)$. This result follows from (1) the lower the EIS, the higher investment result (as shown in panel C in Figure O-7) and (2) the lower the EIS, the higher damage $\ell(\pi)$ (as shown in panel B of Figure O-8.)

Note that the effects of the EIS on the interest rate is ambiguous, which depends on the agent’s belief (panel B). Panel C of Figure O-9 shows the higher the EIS, the lower mitigation in equilibrium the higher risk premium.

OC.2. Disaster Arrival Rate λ_B in State B

In Figure O-10, we plot the first-best solutions for three levels of the disaster arrival rate in state B: $\lambda_B = 0.4, 0.8, 1$. Panel A shows that the higher the disaster arrival rate λ_B in state B, the higher the public mitigation spending x^d . Moreover, the more pessimistic the agent’s belief the stronger this effect. Note that the wedge between the lines for two different levels of λ widens as π increases.

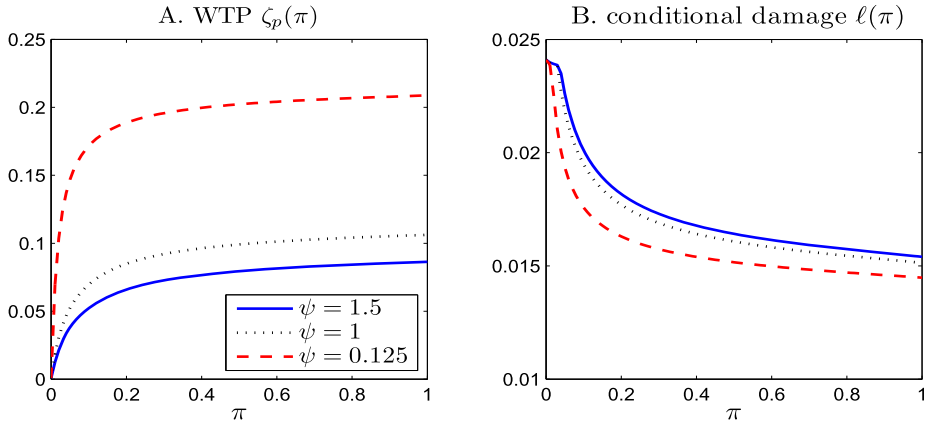


FIGURE O-8.—This figure plots the planner’s first-best solution for three values of the EIS ψ : $1/\gamma = 0.125, 1, 1.5$ for our baseline learning model (with Epstein–Zin utility). The other parameter values are given in Table 4.

Panel B shows that increasing the arrival rate λ_B has a highly nonlinear effect on the private mitigation spending \mathbf{x}^e . Increasing λ_B from 0.4 to 0.8 significantly increases the mitigation spending (for sufficiently large values of π .) However, further increasing λ_B from 0.8 to 1 has limited effects on the mitigation spending. Panel C shows that as λ_B increases, investment falls. The higher the belief level π (the more pessimistic the agent), the larger the impact of λ_B on \mathbf{i} . Panel D shows that the impact of λ_B on consumption \mathbf{c} is ambiguous due to the general equilibrium effect.

In Figure O-11, we show that λ_B has a large effect on the WTP ζ_p (panel A). For example, when the belief changes from $\pi = 0$ to $\pi = 1$, the WTP increases from about 0 to 13% when $\lambda_B = 1$. In contrast, when $\lambda_B = 0.4$, the WTP barely changes from 0 to 2% in response to the same change of the belief. Panel B shows that the higher the arrival rate λ_B the smaller the conditional damage $\ell(\pi)$. This is intuitive as mitigation spending is higher when λ_B is larger. However, as investment is lower when λ_B is larger, the impact of λ_B on the growth rate $\mathbf{g}(\pi)$ is minimal as the two channels (investment and conditional damage) offset each other (panel C). Panel D shows that the higher the arrival rate λ_B , the lower Tobin’s \mathbf{q} , tracking the impact of λ_B on $\mathbf{i}(\pi)$ as $\mathbf{q}(\pi) = 1 + \theta \mathbf{i}(\pi)$. Panel E and

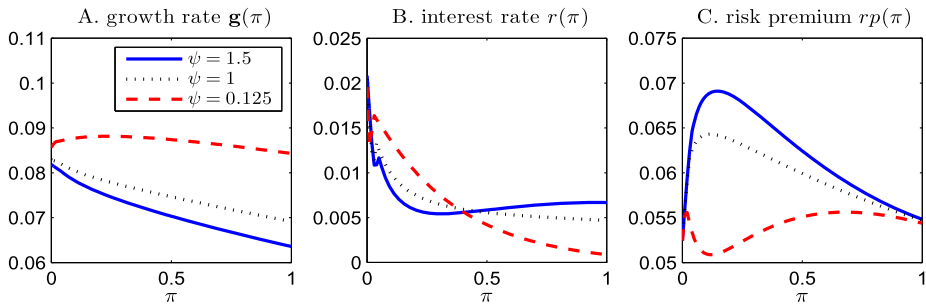


FIGURE O-9.—This figure plots the planner’s first-best solution for three values of the EIS ψ : $1/\gamma = 0.125, 1, 1.5$ for our baseline learning model (with Epstein–Zin utility). The other parameter values are given in Table 4.

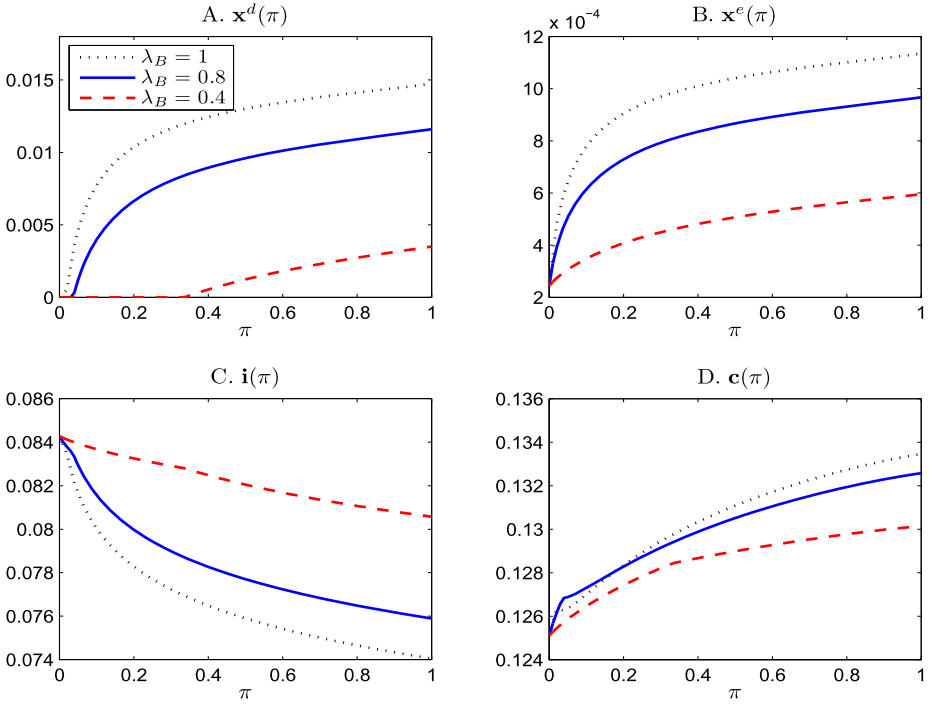


FIGURE O-10.—This figure plots the planner’s first-best solution for three values of the annual disaster arrival rate λ_B : 0.4, 0.8, 1 for our baseline learning model (with Epstein–Zin utility). The other parameter values are given in Table 4.

panel F show that the quantitative effects of λ_B on the risk-free rate r and the market risk premium rp are moderate at best.

OC.3. Time Rate of Preference ρ

In our baseline calculation, we set the time rate of preference ρ at 5% per annum, a commonly used value. Next, we compare our baseline model results with two other economies with lower discount rates: $\rho = 4.5\%$ and $\rho = 6\%$.

Panels A and B of Figure O-12 show that the higher the time rate of preference ρ , the less the planner spends on both types of mitigation spendings, x^d and x^e . Similarly, panel C of Figure O-12 shows that the higher the time rate of preference ρ , the less the planner invests and panel D shows that the higher the time rate of preference ρ the more the agent consumes. The quantitative effects on consumption are large. For example, increasing ρ from 4.5% to 6% roughly increases consumption c from 12% to 15% per annum.

In Figure O-13, we show that the quantitative effects of the time rate of preference ρ on the WTP is significant (panel A). For example, when we change from $\pi = 0$ to $\pi = 1$, the WTP increases from about 0 to 6.7% when $\rho = 6\%$, and increases from 0 to 10% when $\rho = 4.5\%$.

The higher the time rate of preference ρ , the higher the conditional damage $\ell(\pi)$ (panel B) and the lower the Tobin’s q (panel D) as the agent is less patient and puts a smaller weight on the future. Since these two forces push toward the same direction, the higher the discount rate ρ , the lower growth rate g (panel C).

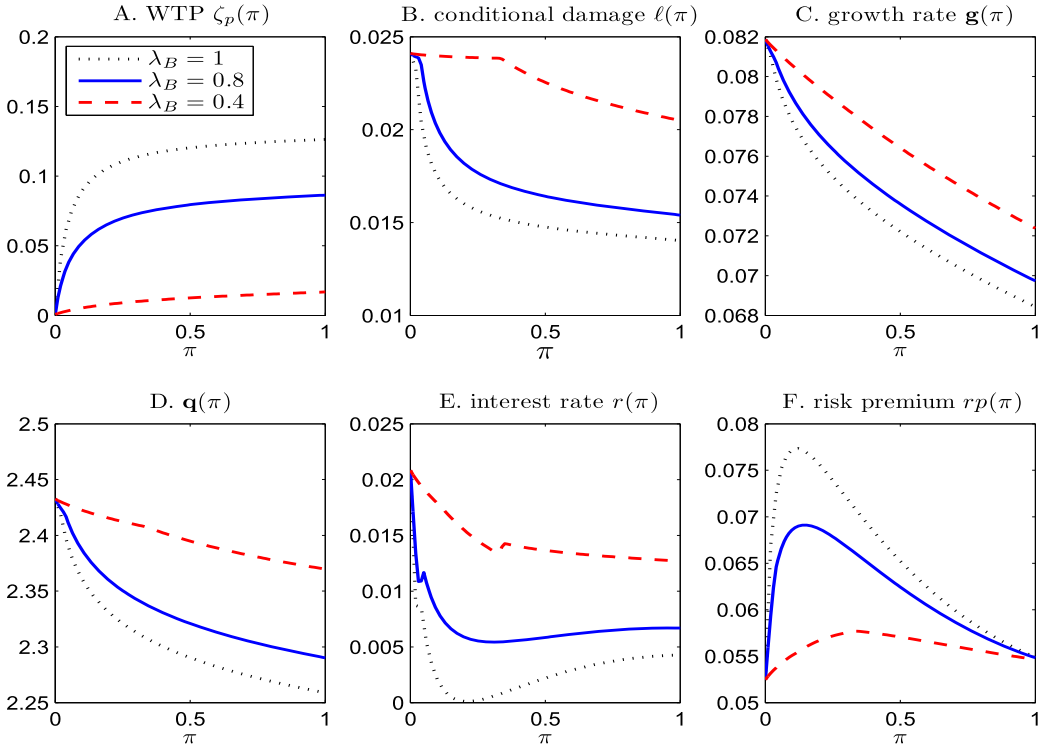


FIGURE O-11.—This figure plots the planner’s first-best solution for three values of the annual disaster arrival rate λ_B : 0.4, 0.8, 1 for our baseline learning model (with Epstein–Zin utility). The other parameter values are given in Table 4.

Finally, panel E shows that the quantitative effect of ρ on the risk-free rate r is moderate at best and panel F shows that the effect of ρ on the market risk premium rp is very small.

OC.4. Coefficient of Relative Risk Aversion γ

In our baseline calculation, we set the coefficient of relative risk aversion γ at 8, which is within the range of widely used values (e.g., 2 to 10). Next, we compare our baseline model results to two other economies with $\gamma = 4$ and $\gamma = 10$.

Panel A of Figure O-14 shows that the higher the coefficient of relative risk aversion γ , the more the planner spends on distribution mitigation \mathbf{x}^d and the less the planner spends on exposure mitigation \mathbf{x}^e . The higher the coefficient of relative risk aversion γ , the less the planner invests (panel C), the more the agent consumes (panel D).

In Figure O-15, we show that the quantitative effects of increasing risk aversion from $\gamma = 4$ to $\gamma = 10$ on the WTP is large (panel A). For example, as we increase γ from 4 to 10, the WTP ζ_p increases from 6.6% to 9.8% when the agent’s belief is $\pi = 1$.

The higher the coefficient of relative risk aversion γ , the lower the conditional damage $\ell(\pi)$ (panel B of Figure O-15) and the lower the growth rate $\mathbf{g}(\pi)$ (panel C of Figure O-15). This is because a more risk-averse agent mitigates more but invests less. Quantitatively, the negative effect of increasing γ via investment on growth dominates the positive

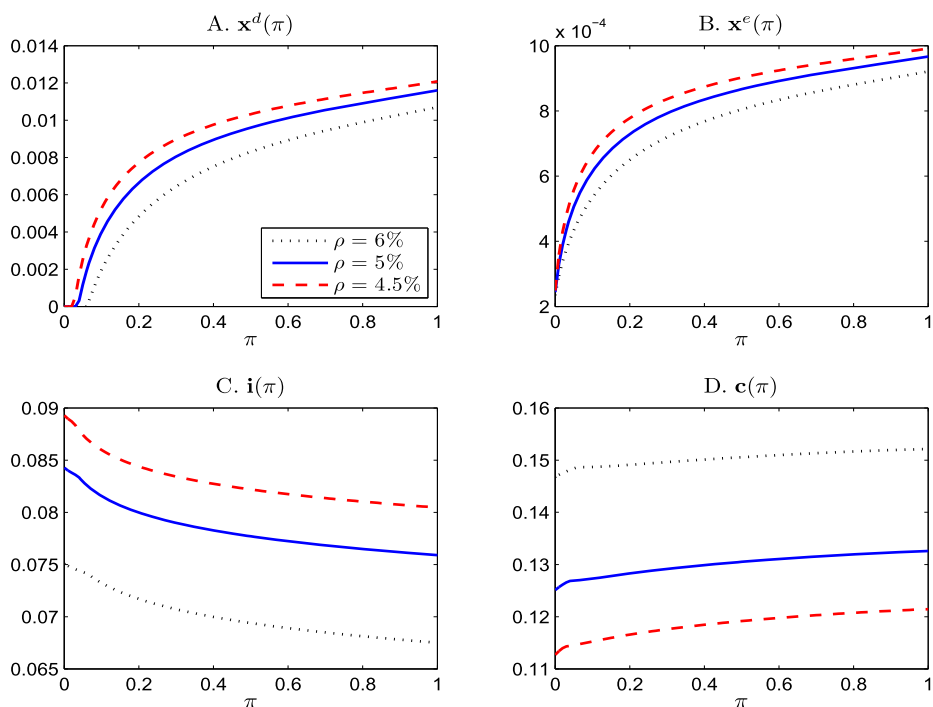


FIGURE O-12.—This figure plots the planner’s first-best solution for three values of the annual time rate of preference ρ : 4.5%, 5%, 6% for our baseline learning model (with Epstein–Zin utility). The other parameter values are given in Table 4.

effect of increasing γ via mitigation. As a result, the net effect of increasing γ on growth is negative.

Finally, panels E and F of Figure O-15 show that the quantitative effects of γ on the risk-free rate r and the market risk premium rp are very large, as we expect (in line with standard asset pricing results).

In Figure O-16, we show the quantitative effects of changing the adjustment cost θ . In panel A, we find that the amount that the planner spends on adaptation is not sensitive to changes in this parameter. In panel B, we find that the amount that firms spend on adaptation spending is also not sensitive to changes in this parameter. In panel C, we find that the amount of investment is highly sensitive to adjustment cost. This is not surprising since increases in adjustment cost of capital directly affects the net benefits of investment. In panel D, we find that consumption is also highly sensitive to this parameter. The reason is the resources constraint as all the adaptation spendings, investment and consumption have to add up to output each period.

In Figure O-17, we find that WTP (panel A) is insensitive to changes in θ . This is related to the findings in panels A and B from Figure O-16. Since adaptation spending in aggregate does not change much with θ , it follows that conditional damage (panel B) also does not change much. Moreover, the risk premium (panel F) is insensitive to changes in θ . This follows from the insensitivity of adaptation spending from panels A and B of Figure O-16, which directly affect conditional damage from disasters and hence also the risk premium.

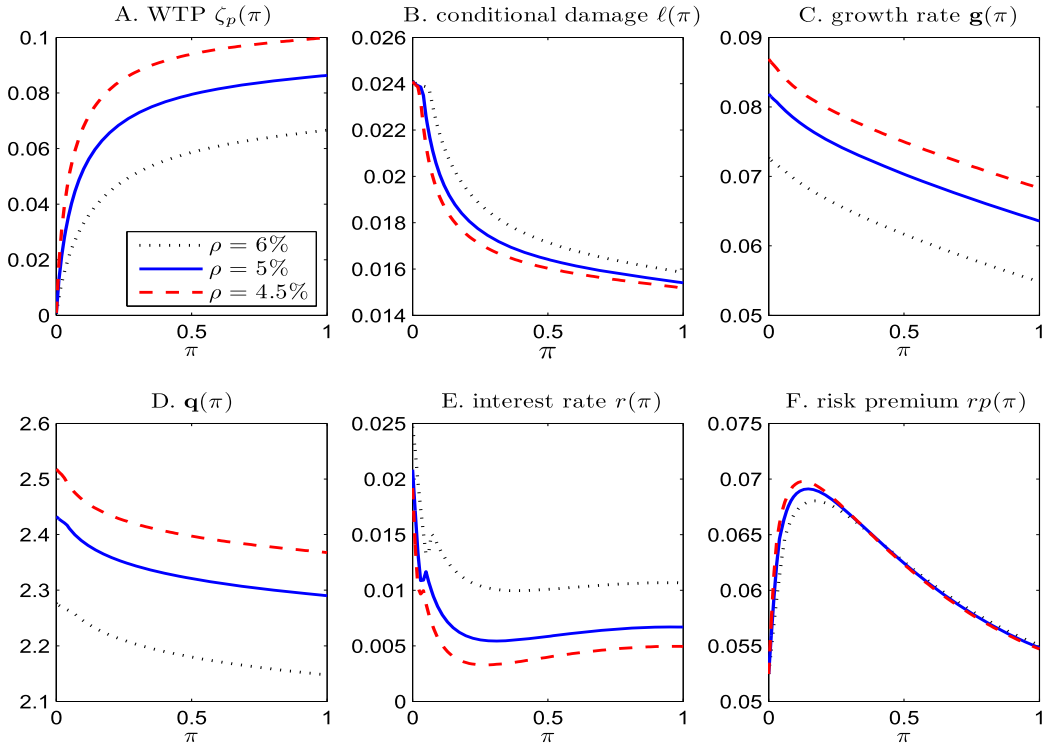


FIGURE O-13.—This figure plots the planner’s first-best solution for three values of the annual time rate of preference ρ : 4.5%, 5%, 6% for our baseline learning model (with Epstein–Zin utility). The other parameter values are given in Table 4.

However, the growth rate (panel C) is sensitive to changes in θ . Since investment is a key driver of growth in the economy, this finding follows from the sensitivity of investment to changes in adjustment cost demonstrated in Figure O-16. Higher adjustment costs naturally also affect Tobin’s q (panel D). Thus we would expect that both of the quantities in panels C and D are sensitive to changes in θ . It turns out that the interest rate (panel E) is also highly sensitive to changes in θ in general equilibrium.

Having done a thorough comparative statics analysis, we next turn to a decomposition of social welfare.

OC.5. Welfare Decomposition

In Figure O-18, we plot the welfare percentage gain, where welfare is measured in terms of willingness to pay (WTP), if we were to transition from our baseline first-best economy with learning (analyzed in Section 3) to various newly constructed economies.

In panel A, the newly constructed economy features no disaster shocks at all, that is, $\lambda_G = \lambda_B = 0$, the percentage gain for the consumer’s WTP (in units of certainty equivalent wealth) increases from about 7% when $\pi = 0$ to about 30% when $\pi = 1$, if the economy transitioned from our baseline economy to this economy with no disaster shocks at all. In panel B, we shut down diffusion shocks in the newly constructed economy by setting $\sigma_K = 0$. The percentage WTP gain decreases from about 43% when $\pi = 0$ to about 39% when $\pi = 1$, if the economy transitioned from our baseline economy to this economy

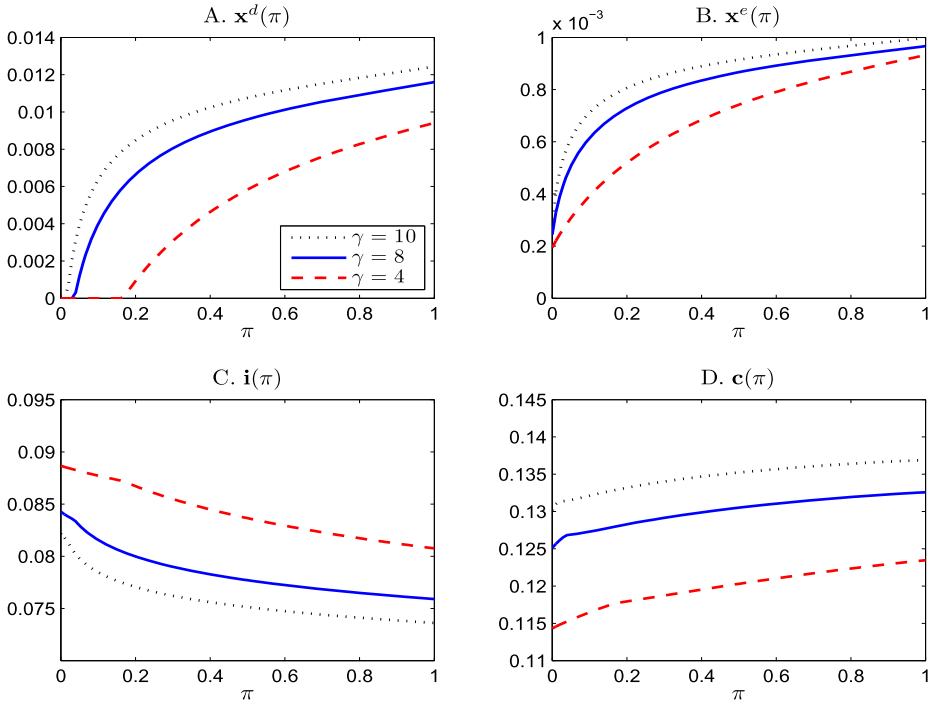


FIGURE O-14.—This figure plots the planner’s first-best solution for three values of coefficient of relative risk aversion γ : 4, 8, 10 for our baseline learning model (with Epstein–Zin utility). The other parameter values are given in Table 4.

with $\sigma_K = 0$. In panel C, the newly constructed economy features neither disaster (jump) shocks nor diffusion shocks, that is, $\lambda_G = \lambda_B = \sigma_K = 0$. The percentage welfare gain for the representative consumer’s WTP increases from about 47% when $\pi = 0$ to about 61% when $\pi = 1$, as we transition from our baseline economy (in Section 2) to this newly constructed economy with no risk at all.

Note that the WTP at $\pi = 1$ for this transition is 61%, lower than the sum of the WTP gain in panel A (30%) and the WTP gain in panel B (39%) by 8%. This more than 10% reduction of the WTP gain is due to the *interaction* between diffusive shocks and jump shocks in our learning model. That is, the total impact on WTP of shutting down both jump shocks ($\lambda_G = \lambda_B = 0$) and diffusion shocks ($\sigma_K = 0$) together is smaller than the sum of (1) the effect on WTP by shutting down the jump shocks ($\lambda_G = \lambda_B = 0$ only) and (2) the effect on WTP by shutting down the diffusion shocks ($\sigma_K = 0$) only.

APPENDIX OD: A GENERALIZED MODEL WITH CARBON STOCK

In this [Appendix](#), we solve our generalized model with carbon stock.

OD.1. *The PDE System*

Using the FOCs and substituting the value function $V(\mathbf{K}, \mathbf{S}, \pi)$ given in (46) into the HJB equation (43), and simplifying the expressions, we obtain the following five-equation

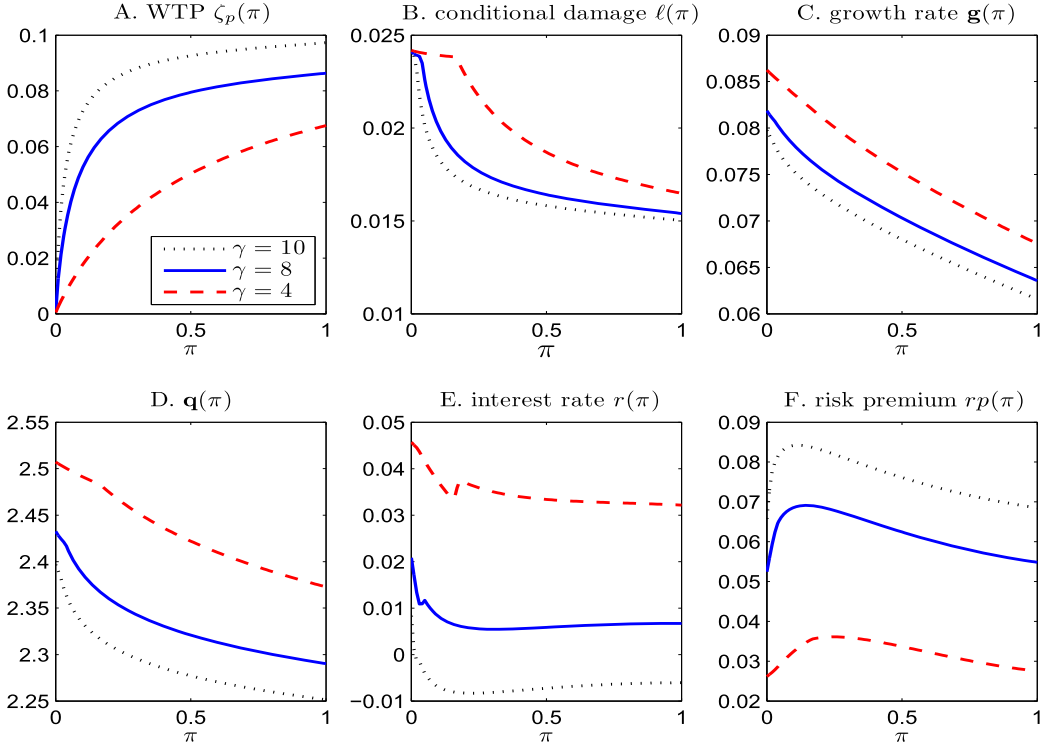


FIGURE O-15.—This figure plots the planner’s first-best solution for three values of the coefficient of relative risk aversion γ : 4, 8, 10 for our baseline learning model (with Epstein–Zin utility). The other parameter values are given in Table 4.

PDE system for $b(\pi, \mathbf{s})$, $\mathbf{i}(\pi, \mathbf{s})$, $\mathbf{x}^d(\pi, \mathbf{s})$, $\mathbf{x}^e(\pi, \mathbf{s})$, and $\mathbf{h}(\pi, \mathbf{s})$:

$$\begin{aligned}
0 = & \frac{\rho}{1 - \psi^{-1}} \left[\left[\frac{b(\pi, \mathbf{s}) - \mathbf{s}b_{\mathbf{s}}(\pi, \mathbf{s})}{\rho(1 + \phi'(\mathbf{i}(\pi, \mathbf{s})))} \right]^{1-\psi} - 1 \right] \\
& + (\mathbf{i}(\pi, \mathbf{s}) - \delta_K) \frac{b(\pi, \mathbf{s}) - \mathbf{s}b_{\mathbf{s}}(\pi, \mathbf{s})}{b(\pi, \mathbf{s})} \\
& - \frac{\gamma\sigma_K^2}{2} + \mu_{\pi}(\pi) \frac{b_{\pi}(\pi, \mathbf{s})}{b(\pi, \mathbf{s})} \\
& + (\mathbf{h}(\pi, \mathbf{s}) - \delta_S \mathbf{s} + \gamma(\sigma_K^2 - \vartheta\sigma_K\sigma_S)\mathbf{s}) \frac{b_{\mathbf{s}}(\pi, \mathbf{s})}{b(\pi, \mathbf{s})} \\
& + \frac{(\sigma_S^2 - 2\vartheta\sigma_K\sigma_S + \sigma_K^2)\mathbf{s}^2}{2} \left(\frac{b_{\mathbf{ss}}(\pi, \mathbf{s})}{b(\pi, \mathbf{s})} - \gamma \frac{(b_{\mathbf{s}}(\pi, \mathbf{s}))^2}{b(\pi, \mathbf{s})^2} \right) \\
& + \frac{\lambda(\pi)}{1 - \gamma} \left[\mathbb{E}^{\mathbf{x}^d(\pi, \mathbf{s})} \right. \\
& \left. \times \left(\frac{(1 - N(\mathbf{x}^e(\pi, \mathbf{s}))(1 - Z))b(\pi^{\mathcal{J}}, \mathbf{s}^{\mathcal{J}})}{b(\pi, \mathbf{s})} \right)^{1-\gamma} - 1 \right], \quad (\text{OD.16})
\end{aligned}$$

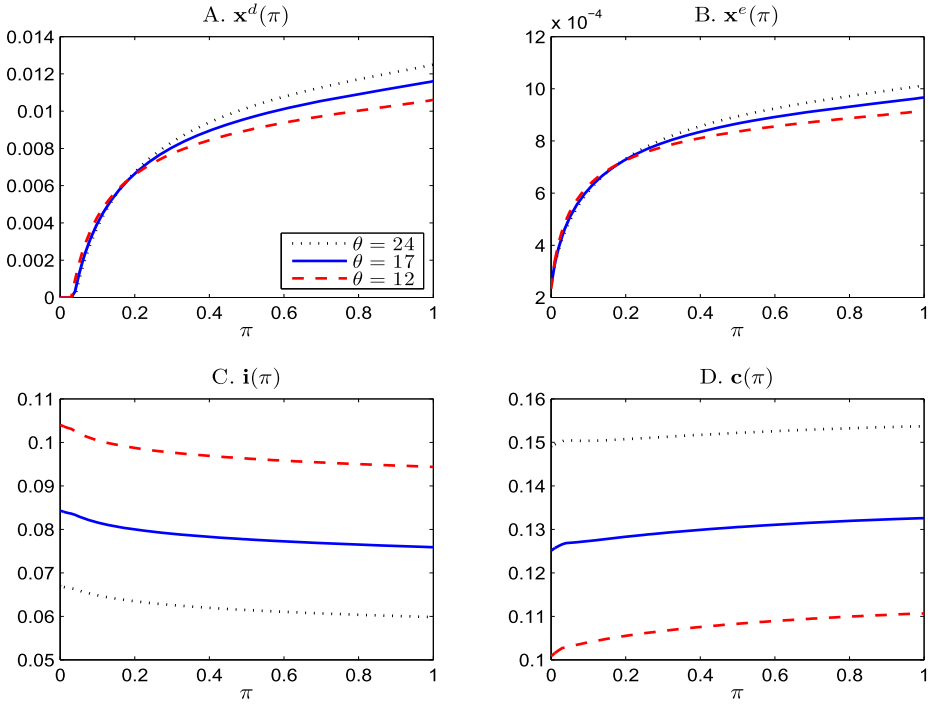


FIGURE O-16.—This figure plots the planner's first-best solution for three values of adjustment cost θ : 12, 17, 24 for our baseline learning model (with Epstein–Zin utility). The other parameter values are given in Table 4.

$$\begin{aligned}
 b(\pi, \mathbf{s}) &= [A\mathbf{h}(\pi, \mathbf{s})^{1-\alpha} - \mathbf{i}(\pi, \mathbf{s}) - \phi(\mathbf{i}(\pi, \mathbf{s})) \\
 &\quad - \mathbf{x}^d(\pi, \mathbf{s}) - \mathbf{x}^e(\pi, \mathbf{s}) - p_H \mathbf{h}(\pi, \mathbf{s})]^{1/(1-\psi)} \\
 &\quad \times \left[\rho(1 + \phi'(\mathbf{i}(\pi, \mathbf{s}))) \frac{b(\pi, \mathbf{s})}{b(\pi, \mathbf{s}) - sb_s(\pi, \mathbf{s})} \right]^{-\psi/(1-\psi)}, \quad (\text{OD.17})
 \end{aligned}$$

$$\frac{b_s(\pi, \mathbf{s})}{b(\pi, \mathbf{s}) - sb_s(\pi, \mathbf{s})} = \frac{p_H - (1 - \alpha)A\mathbf{h}(\pi, \mathbf{s})^{-\alpha}}{1 + \phi'(\mathbf{i}(\pi, \mathbf{s}))}, \quad (\text{OD.18})$$

$$\begin{aligned}
 \frac{1}{1 + \phi'(\mathbf{i}(\pi, \mathbf{s}))} &= \lambda(\pi) \mathbb{E}^{\mathbf{x}^d(\pi, \mathbf{s})} \left[\frac{(Z - 1)N'(\mathbf{x}^e(\pi, \mathbf{s})) (b(\pi^{\mathcal{J}}, \mathbf{s}^{\mathcal{J}}) - \mathbf{s}^{\mathcal{J}} b_s(\pi^{\mathcal{J}}, \mathbf{s}^{\mathcal{J}}))}{b(\pi, \mathbf{s})} \right. \\
 &\quad \left. \times \left(\frac{(1 - N(\mathbf{x}^e(\pi, \mathbf{s}))(1 - Z))b(\pi^{\mathcal{J}}, \mathbf{s}^{\mathcal{J}})}{b(\pi, \mathbf{s})} \right)^{-\gamma} \right], \quad (\text{OD.19})
 \end{aligned}$$

$$\begin{aligned}
 \frac{1}{1 + \phi'(\mathbf{i}(\pi, \mathbf{s}))} &= \frac{\lambda(\pi)}{1 - \gamma} \int_0^1 \left[\frac{\partial \xi(Z; \mathbf{x}^d(\pi, \mathbf{s}))}{\partial \mathbf{x}^d} \right. \\
 &\quad \left. \times \left(\frac{(1 - N(\mathbf{x}^e(\pi, \mathbf{s}))(1 - Z))b(\pi^{\mathcal{J}}, \mathbf{s}^{\mathcal{J}})}{b(\pi, \mathbf{s})} \right)^{1-\gamma} \right] dZ, \quad (\text{OD.20})
 \end{aligned}$$

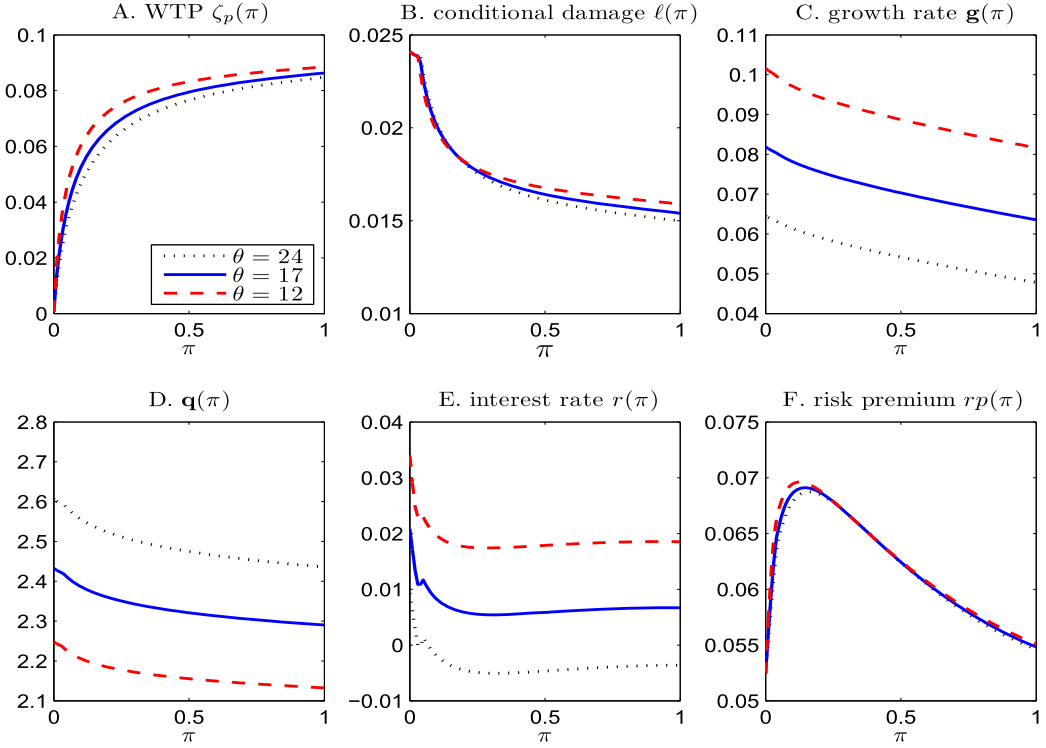


FIGURE O-17.—This figure plots the planner’s first-best solution for three values of adjustment cost θ : 12, 17, 24 for our baseline learning model (with Epstein–Zin utility). The other parameter values are given in Table 4.

where $\mathbf{s}^{\mathcal{J}} = \frac{\mathbf{s}}{1-N(\mathbf{x}^e(\pi, \mathbf{s}))(1-Z)}$ is the post-jump carbon-stock-to-productive-capital ratio \mathbf{s} .⁹

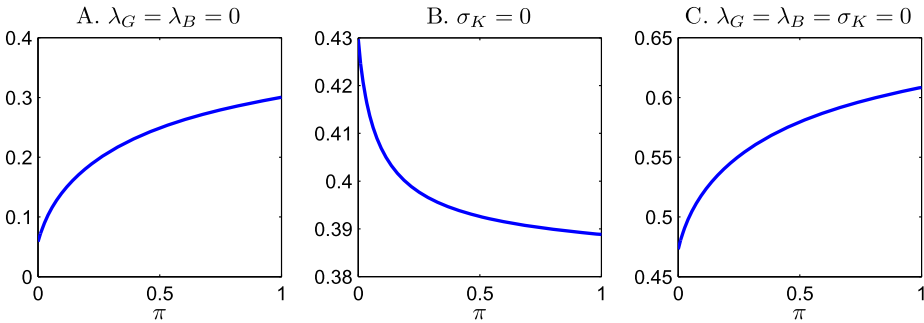


FIGURE O-18.—**Willingness-to-pay (WTP) calculations.** Panel A plots the WTP percentage gain by changing $\lambda_G = 0.1$ and $\lambda_B = 0.8$ to $\lambda_B = \lambda_G = 0$. Panel B plots the WTP percentage gain by changing $\sigma_K = 8\%$ in our baseline economy to $\sigma_K = 0$. Panel C plots the WTP percentage gain by changing $\lambda_G = 0.1$, $\lambda_B = 0.8$, and $\sigma_K = 8\%$ to $\lambda_B = \lambda_G = \sigma_K = 0$.

⁹Recall that \mathbf{s} is a mean-reverting process. Because $\pi = 0$ and $\pi = 1$ are absorbing states, we can obtain the boundary conditions at $\pi = 0$ and $\pi = 1$ by substituting $\pi = 0$ and $\pi = 1$ into (OD.16)–(OD.20).

OD.2. *Competitive Market Equilibrium Solution*

Firm's Optimization Problem. Taking the equilibrium risk-free rate r_t and the market price of (diffusion and jump) risks, the firm maximizes its market value, $Q(K, \pi, \mathbf{s})$ given in (3), where $\{Y_t\}$ is the firm's payout process given in (48).

Applying Ito's lemma to firm value $Q(K, \pi, \mathbf{s}) = q(\pi, \mathbf{s})K$, we obtain

$$\begin{aligned} r(\pi, \mathbf{s})q(\pi, \mathbf{s}) &= \max_{i, x^e, x^d, h} Ah^{1-\alpha} - p_H h - i - \phi(i) - x^e - x^d \\ &\quad + (i - \delta_K - \eta_M^k(\pi, \mathbf{s})\sigma_K)q(\pi, \mathbf{s}) \\ &\quad + \mu_\pi(\pi)q_\pi + \frac{(\sigma_S^2 - 2\vartheta\sigma_S\sigma_K + \sigma_K^2)\mathbf{s}^2}{2}q_{ss} \\ &\quad + [\mu_s(\pi, \mathbf{s}) + \vartheta\sigma_S\sigma_K - \sigma_K^2 - (\eta_M^s(\pi, \mathbf{s})\vartheta\sigma_S - \eta_M^k(\pi, \mathbf{s})\sigma_K)]\mathbf{s}q_s \\ &\quad + \lambda(\pi)\mathbb{E}^{x^d}[\eta(\pi, \mathbf{s}; Z, \mathbf{x}^e)(q(\pi^\mathcal{J}, \mathbf{s}^\mathcal{J})(1 - N(x^e)(1 - Z)) - q(\pi, \mathbf{s}))]. \end{aligned}$$

Note that $x^d = 0$ as no firm spends on public mitigation. The FOCs for i and x^e are

$$\begin{aligned} q(\pi, \mathbf{s}) &= 1 + \phi'(i(\pi, \mathbf{s})), \\ 1 &= -\lambda(\pi)\mathbb{E}^{x^d}[(1 - Z)\eta(\pi, \mathbf{s}; Z, \mathbf{x}^e)q(\pi^\mathcal{J}, \mathbf{s}^\mathcal{J})N'(x^e)]. \end{aligned} \tag{OD.21}$$

We have a new FOC for the firm's fossil fuel usage, h , which is

$$(1 - \alpha)Ah(\pi, \mathbf{s})^{-\alpha} = p_H.$$

In equilibrium, the aggregate scaled fossil fuel, $\mathbf{h}(\pi, \mathbf{s})$, is constant and given by

$$\mathbf{h}(\pi, \mathbf{s}) = \left(\frac{(1 - \alpha)A}{p_H} \right)^{\frac{1}{\alpha}}.$$

Household's Optimization Problem. The household maximizes the value function J_t . We show that the value function is $J_t = J(W_t, \pi_t, \mathbf{s}_t)$ is given by

$$J(W, \pi, \mathbf{s}) = \frac{1}{1 - \gamma} (u(\pi, \mathbf{s})W)^{1 - \gamma},$$

where $u(\pi, \mathbf{s})$ is a welfare measure to be determined. The HJB equation is given by

$$\begin{aligned} 0 &= \max_{C, \Gamma, X^e, X^d} f(C, J) + \mu_\pi(\pi)J_\pi + \lambda(\pi) \int_0^1 [J(W^\mathcal{J}, \pi^\mathcal{J}, \mathbf{s}^\mathcal{J}) - J(W, \pi, \mathbf{s})] \xi(Z; \mathbf{x}^d) dZ \\ &\quad + [r(\pi, \mathbf{s})W + (\mu_Q(\pi, \mathbf{s}) - r(\pi, \mathbf{s}))\Gamma - C]J_W + \mu_s(\pi, \mathbf{s})J_s \\ &\quad + \frac{(\sigma_S^2 - 2\vartheta\sigma_S\sigma_K + \sigma_K^2)\mathbf{s}^2 J_{ss}}{2} \\ &\quad + \left(\left(\frac{\mathbf{q}(\pi, \mathbf{s}) - \mathbf{s}q_s(\pi, \mathbf{s})}{\mathbf{q}(\pi, \mathbf{s})} \sigma_K \right)^2 + 2\vartheta \frac{\mathbf{q}(\pi, \mathbf{s}) - \mathbf{s}q_s(\pi, \mathbf{s})}{\mathbf{q}(\pi, \mathbf{s})} \frac{\mathbf{s}q_s(\pi, \mathbf{s})}{\mathbf{q}(\pi, \mathbf{s})} \sigma_K \sigma_S \right) \end{aligned}$$

$$\begin{aligned}
& + \left(\frac{\mathbf{s}\mathbf{q}_s(\pi, \mathbf{s})}{\mathbf{q}(\pi, \mathbf{s})} \sigma_S \right)^2 \Gamma^2 J_{WW} \Big) / 2 \\
& + \left(\frac{\mathbf{s}\mathbf{q}_s(\pi, \mathbf{s})}{\mathbf{q}(\pi, \mathbf{s})} (\sigma_S^2 - \vartheta \sigma_K \sigma_S) + \frac{\mathbf{q}(\pi, \mathbf{s}) - \mathbf{s}\mathbf{q}_s(\pi, \mathbf{s})}{\mathbf{q}(\pi, \mathbf{s})} (\vartheta \sigma_S \sigma_K - \sigma_K^2) \right) \Gamma \mathbf{s} J_{W_s}. \quad (\text{OD.22})
\end{aligned}$$

Next, we show that by optimally choosing a tax on capital stock, a tax on fossil fuel usage, and a tax on investment, the government can attain the first-best outcome.

OD.3. Optimal Taxation in Market Economy Restores First-Best

In this [Appendix](#), we use the second formulation of optimal taxes in the main text, where the planner taxes a firm's fossil fuel usage and investment if they exceed the respective first-best levels. Anticipating that all three taxes are Markovian in \mathbf{s} and π , we write these tax rates as $\tau^x(\pi, \mathbf{s})$, $\tau^h(\pi, \mathbf{s})$, and $\tau^i(\pi, \mathbf{s})$. Applying Itô's lemma to firm value $Q(K_t, \pi_t, \mathbf{s}_t) = q(\pi_t, \mathbf{s}_t)K_t$ and using the SDF \mathbb{M}_t given in (22), we obtain the following HJB equation for $q(\pi_t, \mathbf{s}_t)$:

$$\begin{aligned}
r(\pi, \mathbf{s})q(\pi, \mathbf{s}) & = \max_{i, x^e, x^d, h} Ah^{1-\alpha} - \tau^x(\pi, \mathbf{s}) - \tau^h(\pi, \mathbf{s})(h - \mathbf{h}) \\
& \quad - \tau^i(\pi, \mathbf{s})[i + \phi(i) - (\mathbf{i} + \phi(\mathbf{i}))] \\
& \quad - p_H h - i - \phi(i) - x^e - x^d + (i - \delta_K - \eta_{\mathbb{M}}^k(\pi, \mathbf{s})\sigma_K)q(\pi, \mathbf{s}) \\
& \quad + [\mu_s(\pi, \mathbf{s}) + \vartheta \sigma_S \sigma_K - \sigma_K^2 - (\eta_{\mathbb{M}}^s(\pi, \mathbf{s})\vartheta \sigma_S - \eta_{\mathbb{M}}^k(\pi, \mathbf{s})\sigma_K)]\mathbf{s}q_s \\
& \quad + \frac{(\sigma_S^2 - 2\vartheta \sigma_S \sigma_K + \sigma_K^2)\mathbf{s}^2}{2} q_{ss} + \mu_\pi(\pi)q_\pi \\
& \quad + \lambda(\pi)\mathbb{E}^{x^d}[\eta(\pi, \mathbf{s}; Z, \mathbf{x}^e)(q(\pi^{\mathcal{J}}, \mathbf{s}^{\mathcal{J}})(1 - N(x^e)(1 - Z)) - q(\pi, \mathbf{s}))].
\end{aligned}$$

As in our baseline model, firms have no incentives to spend on disaster distribution adaptation: $x^d = 0$. The FOC for x^e is the same as (OD.21) for the market economy without taxes (Section OD.2). The FOC for h is given by $(1 - \alpha)Ah(\pi, \mathbf{s})^{-\alpha} = p_H + \tau^h(\pi, \mathbf{s})$ and the FOC i is given by $q(\pi, \mathbf{s}) = (1 + \phi'(i(\pi, \mathbf{s}))(1 + \tau^i(\pi, \mathbf{s})))$.

Next, we show that the household's value in the market economy with taxes $J(W_t, \pi_t, \mathbf{s}_t)$ (Section 8.3) equals that in the first-best economy (Section 8.2). Using the equilibrium result in the market economy: $W_t = \mathbf{q}(\pi_t, \mathbf{s}_t)\mathbf{K}_t$, we write $J(W_t, \pi_t, \mathbf{s}_t) = J(\mathbf{q}(\pi_t, \mathbf{s}_t)\mathbf{K}_t, \pi_t, \mathbf{s}_t)$.

Combining the investment FOC, $\mathbf{q}(\pi, \mathbf{s}) = (1 + \phi'(\mathbf{i}(\pi, \mathbf{s})))\frac{b(\pi, \mathbf{s})}{b(\pi, \mathbf{s}) - \mathbf{s}b_s(\pi, \mathbf{s})}$, with the consumption FOC, $\mathbf{c}(\pi, \mathbf{s}) = \rho^\psi u(\pi, \mathbf{s})^{1-\psi} \mathbf{q}(\pi, \mathbf{s}) = (\rho \mathbf{q}(\pi, \mathbf{s}))^\psi [u(\pi, \mathbf{s}) \mathbf{q}(\pi, \mathbf{s})]^{1-\psi}$, we obtain

$$\mathbf{c}(\pi, \mathbf{s}) = \left[\rho(1 + \phi'(\mathbf{i}(\pi, \mathbf{s}))) \frac{b(\pi, \mathbf{s})}{b(\pi, \mathbf{s}) - \mathbf{s}b_s(\pi, \mathbf{s})} \right]^\psi [u(\pi, \mathbf{s}) \mathbf{q}(\pi, \mathbf{s})]^{1-\psi}.$$

Using $b(\pi, \mathbf{s}) = u(\pi, \mathbf{s}) \mathbf{q}(\pi, \mathbf{s})$ and the resource additivity condition, we obtain

$$\begin{aligned}
b(\pi, \mathbf{s}) & = [Ah(\pi, \mathbf{s})^{1-\alpha} - \tau^x(\pi, \mathbf{s}) - \tau^h(\pi, \mathbf{s})(h(\pi, \mathbf{s}) - \mathbf{h}(\pi, \mathbf{s})) \\
& \quad - \tau^i(\pi, \mathbf{s})[i(\pi, \mathbf{s}) + \phi(i(\pi, \mathbf{s})) - (\mathbf{i}(\pi, \mathbf{s}) + \phi(\mathbf{i}(\pi, \mathbf{s})))]
\end{aligned}$$

$$\begin{aligned}
& - p_H h(\pi, \mathbf{s}) - \mathbf{i}(\pi, \mathbf{s}) - \phi(\mathbf{i}(\pi, \mathbf{s})) - \mathbf{x}^e(\pi, \mathbf{s}) \Big]^{1/(1-\psi)} \\
& \times \left[\rho(1 + \phi'(\mathbf{i}(\pi, \mathbf{s}))) \frac{b(\pi, \mathbf{s})}{b(\pi, \mathbf{s}) - s b_s(\pi, \mathbf{s})} \right]^{-\psi/(1-\psi)}. \tag{OD.23}
\end{aligned}$$

Under optimal taxes, (OD.23) is the same as the investment FOC, given in (OD.17), in the first-best economy. This is because (OD.23) summarizes both the consumer's and the firm's FOCs in the market economy with optimal taxes.

OD.4. Asset Prices in the Planner's First-Best Economy

We derive asset-pricing implications in the first-best economy. Using Itô's lemma, we obtain

$$\begin{aligned}
d\mathbf{s}_t &= d\left(\frac{\mathbf{S}_t}{K_t}\right) = \frac{d\mathbf{S}_t}{K_{t-}} - \frac{\mathbf{S}_{t-} dK_t}{K_{t-}^2} + \frac{\mathbf{S}_{t-} dK_t^2}{K_{t-}^3} - \frac{\langle d\mathbf{S}_t, dK_t \rangle}{K_{t-}^2} \\
&= \mu_s(\pi_{t-}, \mathbf{s}_{t-}) dt + \mathbf{s}_{t-} [\sigma_S d\mathcal{W}_t^S - \sigma_K d\mathcal{W}_t^K + N_{t-}(1-Z) d\mathcal{J}_t],
\end{aligned}$$

where $\mu_s(\pi_{t-}, \mathbf{s}_{t-}) = \mathbf{h}_{t-} - (\mathbf{i}_{t-} - \delta_K + \delta_S - \sigma_K^2 + \vartheta \sigma_K \sigma_S) \mathbf{s}_{t-}$. Duffie and Epstein (1992) show that the SDF $\{\mathbb{M}_t : t \geq 0\}$ implied by the planner's solution is given by

$$\mathbb{M}_t = \exp \left[\int_0^t f_V(\mathbf{C}_s, V_s) ds \right] f_C(\mathbf{C}_t, V_t).$$

Using the FOC for investment, the value function, and the resource constraint, we obtain

$$f_C(\mathbf{C}, V) = \frac{1}{1 + \phi'(\mathbf{i}(\pi, \mathbf{s}))} \frac{b(\pi, \mathbf{s}) - s b_s(\pi, \mathbf{s})}{b(\pi, \mathbf{s})} b(\pi, \mathbf{s})^{1-\gamma} \mathbf{K}^{-\gamma} = \frac{1}{\mathbf{q}(\pi, \mathbf{s})} b(\pi, \mathbf{s})^{1-\gamma} \mathbf{K}^{-\gamma},$$

and

$$f_V(\mathbf{C}, V) = \frac{\rho}{1 - \psi^{-1}} \left[\frac{(1 - \omega) \mathbf{C}^{1-\psi^{-1}}}{((1 - \gamma))^{\omega^{-1}}} V^{-\omega} - (1 - \gamma) \right] = -\epsilon(\pi, \mathbf{s}),$$

where $\epsilon(\pi, \mathbf{s}) = -\frac{\rho(1-\gamma)}{1-\psi^{-1}} \left[\left(\frac{\mathbf{c}(\pi, \mathbf{s})}{b(\pi, \mathbf{s})} \right)^{1-\psi^{-1}} \left(\frac{\psi^{-1}-\gamma}{1-\gamma} \right) - 1 \right]$.

Using Itô's lemma and the optimal allocation rules, we obtain

$$\begin{aligned}
\frac{d\mathbb{M}_t}{\mathbb{M}_{t-}} &= -\epsilon(\pi, \mathbf{s}) dt - \gamma [(\mathbf{i}(\pi, \mathbf{s}) - \delta_K) dt + \sigma_K d\mathcal{W}_t^K] \\
&+ \left[(1 - \gamma) \frac{b_\pi(\pi, \mathbf{s})}{b(\pi, \mathbf{s})} - \frac{\mathbf{q}_\pi(\pi, \mathbf{s})}{\mathbf{q}(\pi, \mathbf{s})} \right] \mu_\pi(\pi) dt \\
&+ \left[(1 - \gamma) \frac{b_s(\pi, \mathbf{s})}{b(\pi, \mathbf{s})} - \frac{\mathbf{q}_s(\pi, \mathbf{s})}{\mathbf{q}(\pi, \mathbf{s})} \right] \\
&\times [(\mu_s(\pi, \mathbf{s}) + \mathbf{s} \gamma (\sigma_K^2 - \vartheta \sigma_S \sigma_K)) dt + \sigma_S d\mathcal{W}_t^S - \sigma_K d\mathcal{W}_t^K] \\
&+ \frac{\gamma(\gamma + 1)}{2} \sigma_K^2 dt
\end{aligned}$$

$$\begin{aligned}
& + \frac{(\sigma_S^2 - 2\vartheta\sigma_S\sigma_K + \sigma_K^2)\mathbf{s}^2}{2} \left[(1-\gamma) \left(\frac{b_{ss}}{b} - \frac{\gamma b_s^2}{b^2} - \frac{b_s \mathbf{q}_s}{b \mathbf{q}} \right) - \frac{\mathbf{q}_{ss}}{\mathbf{q}} + \frac{2\mathbf{q}_s^2}{\mathbf{q}^2} \right] dt \\
& + [\eta(\pi, \mathbf{s}; Z, \mathbf{x}^e) - 1] d\mathcal{J}_t,
\end{aligned}$$

where $\eta(\pi, \mathbf{s}; Z, \mathbf{x}^e) = \frac{\mathbf{q}(\pi, \mathbf{s})}{\mathbf{q}(\pi^{\mathcal{J}}, \mathbf{s}^{\mathcal{J}})} \left(\frac{b(\pi^{\mathcal{J}}, \mathbf{s}^{\mathcal{J}})}{b(\pi, \mathbf{s})} \right)^{1-\gamma} (1 - N(\mathbf{x}^e(\pi, \mathbf{s}))(1 - Z))^{-\gamma}$ and $\mathbf{s}^{\mathcal{J}} = \frac{\mathbf{s}}{1 - N(\mathbf{x}^e(\pi, \mathbf{s}))(1 - Z)}$ is the post-jump ratio carbon-productive-capital ratio \mathbf{s} .

As the expected percentage change of \mathbb{M}_t equals $-r_t$ per unit of time (Duffie (2001)), we obtain the following expression for the interest rate:

$$\begin{aligned}
r(\pi, \mathbf{s}) &= \rho + \psi^{-1}(\mathbf{i} - \delta_K) - \frac{\gamma(\psi^{-1} + 1)\sigma_K^2}{2} - \left[(1 - \psi^{-1}) \frac{b_\pi}{b} - \frac{\mathbf{q}_\pi}{\mathbf{q}} \right] \mu_\pi(\pi) \\
& - \left[(1 - \gamma) \frac{b_s}{b} - \frac{\mathbf{q}_s}{\mathbf{q}} \right] (\mu_s(\pi, \mathbf{s}) + \mathbf{s}\gamma(\sigma_K^2 - \vartheta\sigma_S\sigma_K)) \\
& - \lambda(\pi) [\mathbb{E}^{\mathbf{x}^d}(\eta(\pi, \mathbf{s}; Z, \mathbf{x}^e)) - 1] \\
& + (\psi^{-1} - \gamma) \left[(\mathbf{h} - \delta_S \mathbf{s}) \frac{b_s}{b} + \frac{\sigma_S^2 \mathbf{s}^2}{2} \left(\frac{b_{ss}}{b} - \frac{\gamma b_s^2}{b^2} \right) + (1 - \gamma) \vartheta \sigma_K \sigma_S \mathbf{s} \frac{b_s}{b} \right] \\
& - \frac{(\sigma_S^2 - 2\vartheta\sigma_S\sigma_K + \sigma_K^2)\mathbf{s}^2}{2} \left[(1 - \gamma) \left(\frac{b_{ss}}{b} - \frac{\gamma b_s^2}{b^2} - \frac{b_s \mathbf{q}_s}{b \mathbf{q}} \right) - \frac{\mathbf{q}_{ss}}{\mathbf{q}} + \frac{2\mathbf{q}_s^2}{\mathbf{q}^2} \right] \\
& - \lambda(\pi) \left[\frac{\psi^{-1} - \gamma}{1 - \gamma} \left(1 - \mathbb{E}^{\mathbf{x}^d} \left(\left(\frac{(1 - N(\mathbf{x}^e)(1 - Z))b(\pi^{\mathcal{J}}, \mathbf{s}^{\mathcal{J}})}{b(\pi, \mathbf{s})} \right)^{1-\gamma} \right) \right) \right].
\end{aligned}$$

Applying Itô's lemma to $Q(K, \pi, \mathbf{s}) = q(\pi, \mathbf{s})K$, we obtain the PDE for Tobin's q , $q(\pi, \mathbf{s})$:

$$\begin{aligned}
r(\pi, \mathbf{s})q(\pi, \mathbf{s}) &= A\mathbf{h}^{1-\alpha} - p_H \mathbf{h} - i - \phi(i) - x^e - \mathbf{x}^d \\
& + (i - \delta_K - \eta_{\mathbb{M}}^k(\pi, \mathbf{s})\sigma_K)q(\pi, \mathbf{s}) + \mu_\pi(\pi)q_\pi \\
& + [\mu_s(\pi, \mathbf{s}) + \vartheta\sigma_S\sigma_K - \sigma_K^2 - (\eta_{\mathbb{M}}^s(\pi, \mathbf{s})\vartheta\sigma_S - \eta_{\mathbb{M}}^k(\pi, \mathbf{s})\sigma_K)]\mathbf{s}q_s \\
& + \frac{(\sigma_S^2 - 2\vartheta\sigma_S\sigma_K + \sigma_K^2)\mathbf{s}^2}{2} q_{ss} \\
& + \lambda(\pi) \mathbb{E}^{\mathbf{x}^d} [\eta(\pi, \mathbf{s}; Z, \mathbf{x}^e) (q(\pi^{\mathcal{J}}, \mathbf{s}^{\mathcal{J}}) (1 - N(\mathbf{x}^e)(1 - Z)) - q(\pi, \mathbf{s}))],
\end{aligned}$$

where

$$\eta_{\mathbb{M}}^k(\pi, \mathbf{s}) = \gamma\sigma_K + \left[(1 - \gamma) \frac{\mathbf{s}b_s(\pi, \mathbf{s})}{b(\pi, \mathbf{s})} - \frac{\mathbf{s}\mathbf{q}_s(\pi, \mathbf{s})}{\mathbf{q}(\pi, \mathbf{s})} \right] (\sigma_K - \vartheta\sigma_S)$$

and

$$\eta_{\mathbb{M}}^s(\pi, \mathbf{s}) = \gamma\sigma_K + \left[(1 - \gamma) \frac{\mathbf{s}b_s(\pi, \mathbf{s})}{b(\pi, \mathbf{s})} - \frac{\mathbf{s}\mathbf{q}_s(\pi, \mathbf{s})}{\mathbf{q}(\pi, \mathbf{s})} \right] \left(\sigma_K - \frac{\sigma_S}{\vartheta} \right).$$

Finally, using the equilibrium conditions $q(\pi, \mathbf{s}) = \mathbf{q}(\pi, \mathbf{s})$ and $x^e(\pi, \mathbf{s}) = \mathbf{x}^e(\pi, \mathbf{s})$, we write

$$\begin{aligned} \frac{d\mathbf{Q}_t + \mathbf{D}_{t-} dt}{\mathbf{Q}_{t-}} &= \left(\mu_{\mathbf{Q}}(\pi_{t-}, \mathbf{s}_{t-}) + \lambda(\pi_{t-}) \left(\frac{\mathbf{Q}_t^{\mathcal{J}}}{\mathbf{Q}_{t-}} - 1 \right) \right) dt + \sigma_K d\mathcal{W}_t^K \\ &\quad + \frac{\mathbf{s}_{t-} \mathbf{q}_s(\pi_{t-}, \mathbf{s}_{t-})}{\mathbf{q}(\pi_{t-}, \mathbf{s}_{t-})} [\sigma_S d\mathcal{W}_t^S - \sigma_K d\mathcal{W}_t^K] + \left(\frac{\mathbf{Q}_t^{\mathcal{J}}}{\mathbf{Q}_{t-}} - 1 \right) (d\mathcal{J}_t - \lambda(\pi_{t-}) dt), \end{aligned}$$

where $\frac{\mathbf{Q}_t^{\mathcal{J}}}{\mathbf{Q}_{t-}} = \frac{(1-N(x_{t-}^e)(1-Z))\mathbf{q}(\pi_{t-}^{\mathcal{J}}, \mathbf{s}_{t-}^{\mathcal{J}})}{\mathbf{q}(\pi_{t-}, \mathbf{s}_{t-})}$ and

$$\begin{aligned} \mu_{\mathbf{Q}}(\pi_{t-}, \mathbf{s}_{t-}) &= r(\pi_{t-}, \mathbf{s}_{t-}) + \eta_{\mathbb{M}}^k(\pi_{t-}, \mathbf{s}_{t-})\sigma_K + (\eta_{\mathbb{M}}^s(\pi_{t-}, \mathbf{s}_{t-})\vartheta\sigma_S \\ &\quad - \eta_{\mathbb{M}}^k(\pi_{t-}, \mathbf{s}_{t-})\sigma_K) \frac{\mathbf{s}_{t-} \mathbf{q}_s(\pi_{t-}, \mathbf{s}_{t-})}{\mathbf{q}(\pi_{t-}, \mathbf{s}_{t-})} \\ &\quad + \lambda(\pi_{t-}) \mathbb{E}^{\mathbf{x}_{t-}^d} \left[\eta(\pi_{t-}, \mathbf{s}_{t-}; Z, \mathbf{x}_{t-}^e) \left(1 - \frac{\mathbf{Q}_t^{\mathcal{J}}}{\mathbf{Q}_{t-}} \right) \right]. \end{aligned}$$

The market risk premium is given by

$$\begin{aligned} \text{rp}(\pi_{t-}, \mathbf{s}_{t-}) &= \eta_{\mathbb{M}}^k(\pi_{t-}, \mathbf{s}_{t-})\sigma_K + (\eta_{\mathbb{M}}^s(\pi_{t-}, \mathbf{s}_{t-})\vartheta\sigma_S - \eta_{\mathbb{M}}^k(\pi_{t-}, \mathbf{s}_{t-})\sigma_K) \frac{\mathbf{s}_{t-} \mathbf{q}_s(\pi_{t-}, \mathbf{s}_{t-})}{\mathbf{q}(\pi_{t-}, \mathbf{s}_{t-})} \\ &\quad - \lambda(\pi_{t-}) \mathbb{E}^{\mathbf{x}_{t-}^d} \left[(\eta(\pi_{t-}, \mathbf{s}_{t-}; Z, \mathbf{x}_{t-}^e) - 1) \left(\frac{\mathbf{Q}_t^{\mathcal{J}}}{\mathbf{Q}_{t-}} - 1 \right) \right]. \end{aligned}$$

REFERENCES

- BANSAL, RAVI, AND AMIR YARON (2004): “Risks for the Long Run: A Potential Resolution of Asset Pricing Puzzles,” *Journal of Finance*, 59, 1481–1509. [14]
- CAMPBELL, JOHN Y., AND JOHN H. COCHRANE (1999): “By Force of Habit: A Consumption-Based Explanation of Aggregate Stock Market Behavior,” *Journal of Political Economy*, 107, 205–251. [6,7,11]
- (2015): “The Fragile Benefits of Endowment Destruction,” *Journal of Political Economy*, 123, 1214–1226. [7]
- DUFFIE, DARRELL (2001): *Dynamic Asset Pricing Theory*. Princeton: Princeton University Press. [28]
- DUFFIE, DARRELL, AND LARRY G. EPSTEIN (1992): “Stochastic Differential Utility,” *Econometrica*, 60, 353–394. [27]
- GHADERI, MOHAMMAD, METE KILIC, AND SANG B. SEO (2022): “Learning, Slowly Unfolding Disasters, and Asset Prices,” *Journal of Financial Economics*, 143, 527–549. [1]
- JERMANN, URBAN J. (1998): “Asset Pricing in Production Economies,” *Journal of Monetary Economics*, 41, 257–275. [5]
- WACHTER, JESSICA, AND YICHENG ZHU (2021): “A Model of Two Days: Discrete News and Asset Prices,” Working Paper, Wharton School. [1]

Co-editor Alessandro Lizzeri handled this manuscript.

Manuscript received 23 December, 2021; final version accepted 7 May, 2023; available online 1 June, 2023.